

# Algorithms for nonnegative matrix and tensor factorizations: a unified view based on block coordinate descent framework

Jingu Kim · Yunlong He · Haesun Park

Received: 5 September 2012 / Accepted: 17 January 2013  
© The Author(s) 2013. This article is published with open access at Springerlink.com

**Abstract** We review algorithms developed for nonnegative matrix factorization (NMF) and nonnegative tensor factorization (NTF) from a unified view based on the block coordinate descent (BCD) framework. NMF and NTF are low-rank approximation methods for matrices and tensors in which the low-rank factors are constrained to have only nonnegative elements. The nonnegativity constraints have been shown to enable natural interpretations and allow better solutions in numerous applications including text analysis, computer vision, and bioinformatics. However, the computation of NMF and NTF remains challenging and expensive due the constraints. Numerous algorithmic approaches have been proposed to efficiently compute NMF and NTF. The BCD framework in constrained non-linear optimization readily explains the theoretical convergence properties of several efficient NMF and NTF algorithms, which are consistent with experimental observations reported in literature. In addition, we discuss algorithms that do not fit in the BCD framework contrasting them from those based on the BCD framework. With insights acquired from the unified perspective, we also propose efficient algorithms for updating NMF when there is a small change in the reduced dimension or in the data. The effectiveness of the proposed updating algorithms are validated experimentally with synthetic and real-world data sets.

**Keywords** Nonnegative matrix factorization · Nonnegative tensor factorization · Low-rank approximation · Block coordinate descent

---

J. Kim  
Nokia Inc., 200 S. Mathilda Ave, Sunnyvale, CA, USA  
e-mail: jingu.kim@nokia.com

Y. He  
School of Mathematics, Georgia Institute of Technology, Atlanta, GA, USA  
e-mail: heyunlong@gatech.edu

H. Park (✉)  
School of Computational Science and Engineering, Georgia Institute of Technology, Atlanta, GA, USA  
e-mail: hpark@cc.gatech.edu

19 **1 Introduction**

20 Nonnegative matrix factorization (NMF) is a dimension reduction and factor analysis method.  
 21 Many dimension reduction techniques are closely related to the low-rank approximations  
 22 of matrices, and NMF is special in that the low-rank factor matrices are constrained to  
 23 have only nonnegative elements. The nonnegativity reflects the inherent representation of  
 24 data in many application areas, and the resulting low-rank factors lead to physically natural  
 25 interpretations [66]. NMF was first introduced by Paatero and Tapper [74] as positive matrix  
 26 factorization and subsequently popularized by Lee and Seung [66]. Over the last decade,  
 27 NMF has received enormous attention and has been successfully applied to a broad range  
 28 of important problems in areas including text mining [77,85], computer vision [47,69],  
 29 bioinformatics [10,23,52], spectral data analysis [76], and blind source separation [22] among  
 30 many others.

31 Suppose a nonnegative matrix  $\mathbf{A} \in \mathbb{R}^{M \times N}$  is given. When the desired lower dimension  
 32 is  $K$ , the goal of NMF is to find two matrices  $\mathbf{W} \in \mathbb{R}^{M \times K}$  and  $\mathbf{H} \in \mathbb{R}^{N \times K}$  having only  
 33 nonnegative elements such that

$$34 \quad \mathbf{A} \approx \mathbf{W}\mathbf{H}^T. \quad (1)$$

35 According to (1), each data point, which is represented as a column in  $\mathbf{A}$ , can be approximated  
 36 by an additive combination of the nonnegative basis vectors, which are represented as columns  
 37 in  $\mathbf{W}$ . As the goal of dimension reduction is to discover compact representation in the form of  
 38 (1),  $K$  is assumed to satisfy that  $K < \min \{M, N\}$ . Matrices  $\mathbf{W}$  and  $\mathbf{H}$  are found by solving  
 39 an optimization problem defined with Frobenius norm, Kullback-Leibler divergence [67,68],  
 40 or other divergences [24,68]. In this paper, we focus on the NMF based on Frobenius norm,  
 41 which is the most commonly used formulation:

$$42 \quad \min_{\mathbf{W}, \mathbf{H}} f(\mathbf{W}, \mathbf{H}) = \|\mathbf{A} - \mathbf{W}\mathbf{H}^T\|_F^2 \quad (2)$$

43 subject to  $\mathbf{W} \geq 0, \mathbf{H} \geq 0$ .

44 The constraints in (2) mean that all the elements in  $\mathbf{W}$  and  $\mathbf{H}$  are nonnegative. Problem (2)  
 45 is a non-convex optimization problem with respect to variables  $\mathbf{W}$  and  $\mathbf{H}$ , and finding its  
 46 global minimum is NP-hard [81]. A good algorithm therefore is expected to compute a local  
 47 minimum of (2).

48 Our first goal in this paper is to provide an overview of algorithms developed to solve (2)  
 49 from a unifying perspective. Our review is organized based on the block coordinate descent  
 50 (BCD) method in non-linear optimization, within which we show that most successful NMF  
 51 algorithms and their convergence behavior can be explained. Among numerous algorithms  
 52 studied for NMF, the most popular is the multiplicative updating rule by Lee and Seung [67].  
 53 This algorithm has an advantage of being simple and easy to implement, and it has contributed  
 54 greatly to the popularity of NMF. However, slow convergence of the multiplicative updating  
 55 rule has been pointed out [40,71], and more efficient algorithms equipped with stronger  
 56 theoretical convergence property have been introduced. The efficient algorithms are based  
 57 on either the alternating nonnegative least squares (ANLS) framework [53,59,71] or the  
 58 hierarchical alternating least squares (HALS) method [19,20]. We show that these methods  
 59 can be derived using one common framework of the BCD method and then characterize some  
 60 of the most promising NMF algorithms in Sect. 2. Algorithms for accelerating the BCD-based  
 61 methods as well as algorithms that do not fit in the BCD framework are summarized in Sect. 3,  
 62 where we explain how they differ from the BCD-based methods. In the ANLS method, the  
 63 subproblems appear as the nonnegativity constrained least squares (NLS) problems. Much

research has been devoted to design NMF algorithms based on efficient methods to solve the NLS subproblems [18,42,51,53,59,71]. A review of many successful algorithms for the NLS subproblems is provided in Sect. 4 with discussion on their advantages and disadvantages.

Extending our discussion to low-rank approximations of tensors, we show that algorithms for some nonnegative tensor factorization (NTF) can similarly be elucidated based on the BCD framework. Tensors are mathematical objects for representing multidimensional arrays; vectors and matrices are first-order and second-order special cases of tensors, respectively. The canonical decomposition (CANDECOMP) [14] or the parallel factorization (PARAFAC) [43], which we denote by the CP decomposition, is one of the natural extensions of the singular value decomposition to higher order tensors. The CP decomposition with nonnegativity constraints imposed on the loading matrices [19,21,32,54,60,84], which we denote by nonnegative CP (NCP), can be computed in a way that is similar to the NMF computation. We introduce details of the NCP decomposition and summarize its computation methods based on the BCD method in Sect. 5.

Lastly, in addition to providing a unified perspective, our review leads to the realizations of NMF in more dynamic environments. Such a common case arises when we have to compute NMF for several  $K$  values, which is often needed to determine a proper  $K$  value from data. Based on insights from the unified perspective, we propose an efficient algorithm for updating NMF when  $K$  varies. We show how this method can compute NMFs for a set of different  $K$  values with much less computational burden. Another case occurs when NMF needs to be updated efficiently for a data set which keeps changing due to the inclusion of new data or the removal of obsolete data. This often occurs when the matrices represent data from time-varying signals in computer vision [11] or text mining [13]. We propose an updating algorithm which takes advantage of the fact that most of data in two consecutive time steps are overlapped so that we do not have to compute NMF from scratch. Algorithms for these cases are discussed in Sect. 7, and their experimental validations are provided in Sect. 8.

Our discussion is focused on the algorithmic developments of NMF formulated as (2). In Sect. 9, we only briefly discuss other aspects of NMF and conclude the paper.

*Notations:* Notations used in this paper are as follows. A lowercase or an uppercase letter, such as  $x$  or  $X$ , denotes a scalar; a boldface lowercase letter, such as  $\mathbf{x}$ , denotes a vector; a boldface uppercase letter, such as  $\mathbf{X}$ , denotes a matrix; and a boldface Euler script letter, such as  $\mathcal{X}$ , denotes a tensor of order three or higher. Indices typically start from 1 to its uppercase letter: For example,  $n \in \{1, \dots, N\}$ . Elements of a sequence of vectors, matrices, or tensors are denoted by superscripts within parentheses, such as  $\mathbf{X}^{(1)}, \dots, \mathbf{X}^{(N)}$ , and the entire sequence is denoted by  $\{\mathbf{X}^{(n)}\}$ . When matrix  $\mathbf{X}$  is given,  $(\mathbf{X})_i$  or  $\mathbf{x}_i$  denotes its  $i$ th column,  $(\mathbf{X})_i$  or  $\mathbf{x}_i$  denotes its  $i$ th row, and  $x_{ij}$  denotes its  $(i, j)$ th element. For simplicity, we also let  $\mathbf{x}_i$  (without a dot) denote the  $i$ th column of  $\mathbf{X}$ . The set of nonnegative real numbers are denoted by  $\mathbb{R}_+$ , and  $\mathbf{X} \geq 0$  indicates that the elements of  $\mathbf{X}$  are nonnegative. The notation  $[\mathbf{X}]_+$  denotes a matrix that is the same as  $\mathbf{X}$  except that all its negative elements are set to zero. A *nonnegative matrix* or a *nonnegative tensor* refers to a matrix or a tensor with only nonnegative elements. The null space of matrix  $\mathbf{X}$  is denoted by  $\text{null}(\mathbf{X})$ . Operator  $\otimes$  denotes element-wise multiplication of vectors or matrices.

## 2 A unified view—BCD framework for NMF

The BCD method is a divide-and-conquer strategy that can be generally applied to non-linear optimization problems. It divides variables into several disjoint subgroups and iteratively minimize the objective function with respect to the variables of each subgroup at a time.

110 We first introduce the BCD framework and its convergence properties and then explain  
 111 several NMF algorithms under the framework.

112 Consider a constrained non-linear optimization problem:

113 
$$\min f(\mathbf{x}) \text{ subject to } \mathbf{x} \in \mathcal{X}, \tag{3}$$

114 where  $\mathcal{X}$  is a closed convex subset of  $\mathbb{R}^N$ . An important assumption to be exploited in the  
 115 BCD framework is that  $\mathcal{X}$  is represented by a Cartesian product:

116 
$$\mathcal{X} = \mathcal{X}_1 \times \dots \times \mathcal{X}_M, \tag{4}$$

117 where  $\mathcal{X}_m, m = 1, \dots, M$ , is a closed convex subset of  $\mathbb{R}^{N_m}$  satisfying  $N = \sum_{m=1}^M N_m$ .  
 118 Accordingly, vector  $\mathbf{x}$  is partitioned as  $\mathbf{x} = (\mathbf{x}_1, \dots, \mathbf{x}_M)$  so that  $\mathbf{x}_m \in \mathcal{X}_m$  for  $m = 1, \dots, M$ .  
 119 The BCD method solves for  $\mathbf{x}_m$  fixing all other subvectors of  $\mathbf{x}$  in a cyclic manner. That is,  
 120 if  $\mathbf{x}^{(i)} = (\mathbf{x}_1^{(i)}, \dots, \mathbf{x}_M^{(i)})$  is given as the current iterate at the  $i$ th step, the algorithm generates  
 121 the next iterate  $\mathbf{x}^{(i+1)} = (\mathbf{x}_1^{(i+1)}, \dots, \mathbf{x}_M^{(i+1)})$  block by block, according to the solution of the  
 122 following subproblem:

123 
$$\mathbf{x}_m^{(i+1)} \leftarrow \arg \min_{\xi \in \mathcal{X}_m} f \left( \mathbf{x}_1^{(i+1)}, \dots, \mathbf{x}_{m-1}^{(i+1)}, \xi, \mathbf{x}_{m+1}^{(i)}, \dots, \mathbf{x}_M^{(i)} \right). \tag{5}$$

124 Also known as a *non-linear Gauss-Siedel* method [5], this algorithm updates one block  
 125 each time, always using the most recently updated values of other blocks  $\mathbf{x}_{\tilde{m}}, \tilde{m} \neq m$ . This is  
 126 important since it ensures that after each update the objective function value does not increase.  
 127 For a sequence  $\{\mathbf{x}^{(i)}\}$  where each  $\mathbf{x}^{(i)}$  is generated by the BCD method, the following property  
 128 holds.

129 **Theorem 1** Suppose  $f$  is continuously differentiable in  $\mathcal{X} = \mathcal{X}_1 \times \dots \times \mathcal{X}_M$ , where  $\mathcal{X}_m, m =$   
 130  $1, \dots, M$ , are closed convex sets. Furthermore, suppose that for all  $m$  and  $i$ , the minimum of

131 
$$\min_{\xi \in \mathcal{X}_m} f \left( \mathbf{x}_1^{(i+1)}, \dots, \mathbf{x}_{m-1}^{(i+1)}, \xi, \mathbf{x}_{m+1}^{(i)}, \dots, \mathbf{x}_M^{(i)} \right)$$

132 is uniquely attained. Let  $\{\mathbf{x}^{(i)}\}$  be the sequence generated by the BCD method in (5). Then,  
 133 every limit point of  $\{\mathbf{x}^{(i)}\}$  is a stationary point. The uniqueness of the minimum is not required  
 134 when  $M$  is two.

135 The proof of this theorem for an arbitrary number of blocks is shown in Bertsekas [5], and  
 136 the last statement regarding the two-block case is due to Grippo and Sciandrone [41]. For a  
 137 non-convex optimization problem, most algorithms only guarantee the stationarity of a limit  
 138 point [46,71].

139 When applying the BCD method to a constrained non-linear programming problem, it  
 140 is critical to wisely choose a partition of  $\mathcal{X}$ , whose Cartesian product constitutes  $\mathcal{X}$ . An  
 141 important criterion is whether subproblems (5) for  $m = 1, \dots, M$  are efficiently solvable:  
 142 For example, if the solutions of subproblems appear in a closed form, each update can be  
 143 computed fast. In addition, it is worth checking whether the solutions of subproblems depend  
 144 on each other. The BCD method requires that the most recent values need to be used for each  
 145 subproblem (5). When the solutions of subproblems depend on each other, they have to be  
 146 computed sequentially to make use of the most recent values; if solutions for some blocks are  
 147 independent from each other, however, simultaneous computation of them would be possible.  
 148 We discuss how different choices of partitions lead to different NMF algorithms. Three cases  
 149 of partitions are shown in Fig. 1, and each case is discussed below.

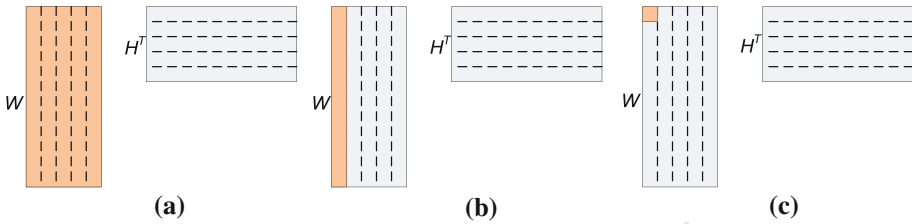


**Fig. 1** Different choices of block partitions for the BCD method for NMF where  $\mathbf{W} \in \mathbb{R}_+^{M \times K}$  and  $\mathbf{H} \in \mathbb{R}_+^{N \times K}$ . In each case, the highlighted part for example is updated fixing all the rest. **a** Two matrix blocks. **b**  $2K$  vector blocks. **c**  $K(M + N)$  scalar blocks

150 2.1 BCD with two matrix blocks—ANLS method

151 In (2), a natural partitioning of the variables is the two blocks representing  $\mathbf{W}$  and  $\mathbf{H}$ , as  
 152 shown in Fig. 1a. In this case, following the BCD method in (5), we take turns solving

153 
$$\mathbf{W} \leftarrow \arg \min_{\mathbf{W} \geq 0} f(\mathbf{W}, \mathbf{H}) \text{ and } \mathbf{H} \leftarrow \arg \min_{\mathbf{H} \geq 0} f(\mathbf{W}, \mathbf{H}). \tag{6}$$

154 These subproblems can be written as

155 
$$\min_{\mathbf{W} \geq 0} \|\mathbf{H}\mathbf{W}^T - \mathbf{A}^T\|_F^2 \text{ and} \tag{7a}$$

156 
$$\min_{\mathbf{H} \geq 0} \|\mathbf{W}\mathbf{H}^T - \mathbf{A}\|_F^2. \tag{7b}$$

157 Since subproblems (7) are the nonnegativity constrained least squares (NLS) problems, the  
 158 two-block BCD method has been called the alternating nonnegative least square (ANLS)  
 159 framework [53, 59, 71]. Even though the subproblems are convex, they do not have a closed-  
 160 form solution, and a numerical algorithm for the subproblem has to be provided. Several  
 161 approaches for solving the NLS subproblems proposed in NMF literature are discussed in  
 162 Sect. 4 [18, 42, 51, 53, 59, 71]. According to Theorem 1, the convergence property of the ANLS  
 163 framework can be stated as follows.

164 **Corollary 1** *If a minimum of each subproblem in (7) is attained at each step, every limit*  
 165 *point of the sequence  $\{(\mathbf{W}, \mathbf{H})^{(i)}\}$  generated by the ANLS framework is a stationary point of*  
 166 *(2).*

167 Note that the minimum is not required to be unique for the convergence result to hold  
 168 because the number of blocks are two [41]. Therefore,  $\mathbf{H}$  in (7a) or  $\mathbf{W}$  in (7b) need not  
 169 be of full column rank for the property in Corollary 1 to hold. On the other hand, some  
 170 numerical methods for the NLS subproblems require the full rank conditions so that they  
 171 return a solution that attains a minimum: See Sect. 4 as well as regularization methods in  
 172 Sect. 2.4.

173 Subproblems (7) can be decomposed into independent NLS problems with a single right-  
 174 hand side vector. For example,

175 
$$\min_{\mathbf{W} \geq 0} \|\mathbf{H}\mathbf{W}^T - \mathbf{A}^T\|_F^2 = \sum_{m=1}^M \min_{\mathbf{w}_m \geq 0} \|\mathbf{H}\mathbf{w}_m^T - \mathbf{a}_m^T\|_F^2, \tag{8}$$

176 and we can solve the problems in the second term independently. This view corresponds to  
 177 a BCD method with  $M + N$  vector blocks, in which each block corresponds to a row of

178 **W** or **H**. In literature, however, this view has not been emphasized because often it is more  
 179 efficient to solve the NLS problems with multiple right-hand sides altogether: See Sect. 4.

180 2.2 BCD with  $2K$  vector blocks—HALS/RRI method

181 Let us now partition the unknowns into  $2K$  blocks in which each block is a column of  
 182 **W** or **H**, as shown in Fig. 1b. In this case, it is easier to consider the objective function in the  
 183 following form:

184 
$$f(\mathbf{w}_1, \dots, \mathbf{w}_K, \mathbf{h}_1, \dots, \mathbf{h}_K) = \left\| \mathbf{A} - \sum_{k=1}^K \mathbf{w}_k \mathbf{h}_k^T \right\|_F^2, \tag{9}$$

185 where  $\mathbf{W} = [\mathbf{w}_1, \dots, \mathbf{w}_K] \in \mathbb{R}_+^{M \times K}$  and  $\mathbf{H} = [\mathbf{h}_1, \dots, \mathbf{h}_K] \in \mathbb{R}_+^{N \times K}$ . The form in (9)  
 186 represents that **A** is approximated by the sum of  $K$  rank-one matrices.

187 Following the BCD scheme, we can minimize  $f$  by iteratively solving

188 
$$\mathbf{w}_k \leftarrow \arg \min_{\mathbf{w}_k \geq 0} f(\mathbf{w}_1, \dots, \mathbf{w}_K, \mathbf{h}_1, \dots, \mathbf{h}_K)$$

189 for  $k = 1, \dots, K$ , and

190 
$$\mathbf{h}_k \leftarrow \arg \min_{\mathbf{h}_k \geq 0} f(\mathbf{w}_1, \dots, \mathbf{w}_K, \mathbf{h}_1, \dots, \mathbf{h}_K)$$

191 for  $k = 1, \dots, K$ . These subproblems appear as

192 
$$\min_{\mathbf{w} \geq 0} \|\mathbf{h}_k \mathbf{w}^T - \mathbf{R}_k^T\|_F^2 \text{ and } \min_{\mathbf{h} \geq 0} \|\mathbf{w}_k \mathbf{h}^T - \mathbf{R}_k\|_F^2, \tag{10}$$

193 where

194 
$$\mathbf{R}_k = \mathbf{A} - \sum_{\tilde{k}=1, \tilde{k} \neq k}^K \mathbf{w}_{\tilde{k}} \mathbf{h}_{\tilde{k}}^T. \tag{11}$$

195 A promising aspect of this  $2K$  block partitioning is that each subproblem in (10) has a  
 196 closed-form solution, as characterized in the following theorem.

197 **Theorem 2** Consider a minimization problem

198 
$$\min_{\mathbf{v} \geq 0} \|\mathbf{u} \mathbf{v}^T - \mathbf{G}\|_F^2 \tag{12}$$

199 where  $\mathbf{G} \in \mathbb{R}^{M \times N}$  and  $\mathbf{u} \in \mathbb{R}^M$  are given. If  $\mathbf{u}$  is a nonzero vector,  $\mathbf{v} = \frac{[\mathbf{G}^T \mathbf{u}]_+}{\mathbf{u}^T \mathbf{u}}$  is the unique  
 200 solution for (12), where  $([\mathbf{G}^T \mathbf{u}]_+)_n = \max((\mathbf{G}^T \mathbf{u})_n, 0)$  for  $n = 1, \dots, N$ .

201 *Proof* Letting  $\mathbf{v}^T = (v_1, \dots, v_N)$ , we have

202 
$$\min_{\mathbf{v} \geq 0} \|\mathbf{u} \mathbf{v}^T - \mathbf{G}\|_F^2 = \sum_{n=1}^N \min_{v_n \geq 0} \|\mathbf{u} v_n - \mathbf{g}_n\|_2^2,$$

203 where  $\mathbf{G} = [\mathbf{g}_1, \dots, \mathbf{g}_N]$ , and the problems in the second term are independent of each other.  
 204 Let  $h(v_n) = \|\mathbf{u} v_n - \mathbf{g}_n\|_2^2 = \|\mathbf{u}\|_2^2 v_n^2 - 2v_n \mathbf{u}^T \mathbf{g}_n + \|\mathbf{g}_n\|_2^2$ . Since  $\frac{\partial h}{\partial v_n} = 2(v_n \|\mathbf{u}\|_2^2 - \mathbf{g}_n^T \mathbf{u})$ ,  
 205 if  $\mathbf{g}_n^T \mathbf{u} \geq 0$ , it is clear that the minimum value of  $h(v_n)$  is attained at  $v_n = \frac{\mathbf{g}_n^T \mathbf{u}}{\mathbf{u}^T \mathbf{u}}$ . If  $\mathbf{g}_n^T \mathbf{u} < 0$ ,  
 206 the value of  $h(v_n)$  increases as  $v_n$  becomes larger than zero, and therefore the minimum is  
 207 attained at  $v_n = 0$ . Combining the two cases, the solution can be expressed as  $v_n = \frac{[\mathbf{g}_n^T \mathbf{u}]_+}{\mathbf{u}^T \mathbf{u}}$ .  
 208  $\square$

209 Using Theorem 2, the solutions of (10) can be stated as

$$210 \quad \mathbf{w}_k \leftarrow \frac{[\mathbf{R}_k \mathbf{h}_k]_+}{\|\mathbf{h}_k\|_2^2} \quad \text{and} \quad \mathbf{h}_k \leftarrow \frac{[\mathbf{R}_k^T \mathbf{w}_k]_+}{\|\mathbf{w}_k\|_2^2}. \quad (13)$$

211 This  $2K$ -block BCD algorithm has been studied under the name of the hierarchical alternating  
 212 least squares (HALS) method by Cichocki et al. [19,20] and the rank-one residue iteration  
 213 (RRI) independently by Ho [44]. According to Theorem 1, the convergence property of the  
 214 HALS/RRI algorithm can be written as follows.

215 **Corollary 2** *If the columns of  $\mathbf{W}$  and  $\mathbf{H}$  remain nonzero throughout all the iterations and*  
 216 *the minimums in (13) are attained at each step, every limit point of the sequence  $\{(\mathbf{W}, \mathbf{H})^{(i)}\}$*   
 217 *generated by the HALS/RRI algorithm is a stationary point of (2).*

218 In practice, a zero column could occur in  $\mathbf{W}$  or  $\mathbf{H}$  during the HALS/RRI algorithm. This  
 219 happens if  $\mathbf{h}_k \in \text{null}(\mathbf{R}_k)$ ,  $\mathbf{w}_k \in \text{null}(\mathbf{R}_k^T)$ ,  $\mathbf{R}_k \mathbf{h}_k \leq 0$ , or  $\mathbf{R}_k^T \mathbf{w}_k \leq 0$ . To prevent zero  
 220 columns, a small positive number could be used for the maximum operator in (13): That is,  
 221  $\max(\cdot, \epsilon)$  with a small positive number  $\epsilon$  such as  $10^{-16}$  is used instead of  $\max(\cdot, 0)$  [20,35].  
 222 The HALS/RRI algorithm with this modification often shows faster convergence compared to  
 223 other BCD methods or previously developed methods [37,59]. See Sect. 3.1 for acceleration  
 224 techniques for the HALS/RRI method and Sect. 6.2 for more discussion on experimental  
 225 comparisons.

226 For an efficient implementation, it is not necessary to explicitly compute  $\mathbf{R}_k$ . Replacing  
 227  $\mathbf{R}_k$  in (13) with the expression in (11), the solutions can be rewritten as

$$228 \quad \mathbf{w}_k \leftarrow \left[ \mathbf{w}_k + \frac{(\mathbf{A}\mathbf{H})_{\cdot k} - (\mathbf{W}\mathbf{H}^T \mathbf{H})_{\cdot k}}{(\mathbf{H}^T \mathbf{H})_{kk}} \right]_+ \quad \text{and} \quad (14a)$$

$$229 \quad \mathbf{h}_k \leftarrow \left[ \mathbf{h}_k + \frac{(\mathbf{A}^T \mathbf{W})_{\cdot k} - (\mathbf{H}\mathbf{W}^T \mathbf{W})_{\cdot k}}{(\mathbf{W}^T \mathbf{W})_{kk}} \right]_+. \quad (14b)$$

230 The choice of update formulae is related with the choice of an update order. Two versions of  
 231 an update order can be considered:

$$232 \quad \mathbf{w}_1 \rightarrow \mathbf{h}_1 \rightarrow \dots \rightarrow \mathbf{w}_K \rightarrow \mathbf{h}_K \quad (15)$$

233 and

$$234 \quad \mathbf{w}_1 \rightarrow \dots \rightarrow \mathbf{w}_K \rightarrow \mathbf{h}_1 \rightarrow \dots \rightarrow \mathbf{h}_K. \quad (16)$$

235 When using (13), update order (15) is more efficient because  $\mathbf{R}_k$  is explicitly computed and  
 236 then used to update both  $\mathbf{w}_k$  and  $\mathbf{h}_k$ . When using (14), although either (15) or (16) can be used,  
 237 update order (16) tends to be more efficient in environments such as MATLAB based on our  
 238 experience. To update all the elements in  $\mathbf{W}$  and  $\mathbf{H}$ , update formulae (13) with ordering (15)  
 239 require  $8KMN + 3K(M + N)$  floating point operations, whereas update formulae (14) with  
 240 either choice of ordering require  $4KMN + (4K^2 + 6K)(M + N)$  floating point operations.  
 241 When  $K \ll \min(M, N)$ , the latter is more efficient. Moreover, the memory requirement of  
 242 (14) is smaller because  $\mathbf{R}_k$  need not be stored. For more details, see Cichocki and Phan [19].

### 243 2.3 BCD with $K(M + N)$ scalar blocks

244 In one extreme, the unknowns can be partitioned into  $K(M + N)$  blocks of scalars, as shown  
 245 in Fig. 1c. In this case, every element of  $\mathbf{W}$  and  $\mathbf{H}$  is considered as a block in the context

of Theorem 1. To this end, it helps to write the objective function as a quadratic function of scalar  $w_{mk}$  or  $h_{nk}$  assuming all other elements in  $\mathbf{W}$  and  $\mathbf{H}$  are fixed:

$$f(w_{mk}) = \left\| \left( \mathbf{a}_m - \sum_{\tilde{k} \neq k} w_{m\tilde{k}} \mathbf{h}_{\tilde{k}}^T \right) - w_{mk} \mathbf{h}_k^T \right\|_2^2 + \text{const}, \tag{17a}$$

$$f(h_{nk}) = \left\| \left( \mathbf{a}_n - \sum_{\tilde{k} \neq k} w_{n\tilde{k}} h_{n\tilde{k}} \right) - w_{nk} h_{nk} \right\|_2^2 + \text{const}, \tag{17b}$$

where  $\mathbf{a}_m$  and  $\mathbf{a}_n$  denote the  $m$ th row and the  $n$ th column of  $\mathbf{A}$ , respectively. According to the BCD framework, we iteratively update each block by

$$w_{mk} \leftarrow \arg \min_{w_{mk} \geq 0} f(w_{mk}) = \left[ w_{mk} + \frac{(\mathbf{A}\mathbf{H})_{mk} - (\mathbf{W}\mathbf{H}^T\mathbf{H})_{mk}}{(\mathbf{H}^T\mathbf{H})_{kk}} \right]_+ \tag{18a}$$

$$h_{nk} \leftarrow \arg \min_{h_{nk} \geq 0} f(h_{nk}) = \left[ h_{nk} + \frac{(\mathbf{A}^T\mathbf{W})_{nk} - (\mathbf{H}\mathbf{W}^T\mathbf{W})_{nk}}{(\mathbf{W}^T\mathbf{W})_{kk}} \right]_+. \tag{18b}$$

The updates of  $w_{mk}$  and  $h_{nk}$  are independent of all other elements in the same column. Therefore, it is possible to update all the elements in each column of  $\mathbf{W}$  (and  $\mathbf{H}$ ) simultaneously. Once we organize the update of (18) column-wise, the result is the same as (14). That is, a particular arrangement of the BCD method with scalar blocks is equivalent to the BCD method with  $2K$  vector blocks. Accordingly, the HALS/RRI method can be derived by the BCD method either with vector blocks or with scalar blocks. On the other hand, it is not possible to simultaneously solve for the elements in each row of  $\mathbf{W}$  (or  $\mathbf{H}$ ) because their solutions depend on each other. The convergence property of the scalar block case is similar to that of the vector block case.

**Corollary 3** *If the columns of  $\mathbf{W}$  and  $\mathbf{H}$  remain nonzero throughout all the iterations and if the minimums in (18) are attained at each step, every limit point of the sequence  $\{(\mathbf{W}, \mathbf{H})^{(i)}\}$  generated by the BCD method with  $K(M + N)$  scalar blocks is a stationary point of (2).*

The multiplicative updating rule also uses element-wise updating [67]. However, the multiplicative updating rule is different from the scalar block BCD method in a sense that its solutions are not optimal for subproblems (18). See Sect. 3.2 for more discussion.

### 2.4 BCD for some variants of NMF

To incorporate extra constraints or prior information into the NMF formulation in (2), various regularization terms can be added. We can consider an objective function

$$\min_{\mathbf{W}, \mathbf{H} \geq 0} \left\| \mathbf{A} - \mathbf{W}\mathbf{H}^T \right\|_F^2 + \phi(\mathbf{W}) + \psi(\mathbf{H}), \tag{19}$$

where  $\phi(\cdot)$  and  $\psi(\cdot)$  are regularization terms that often involve matrix or vector norms. Here we discuss the Frobenius-norm and the  $l_1$ -norm regularization and show how NMF regularized by those norms can be easily computed using the BCD method. Scalar parameters  $\alpha$  or  $\beta$  in this subsection are used to control the strength of regularization.

The Frobenius-norm regularization [53, 76] corresponds to

$$\phi(\mathbf{W}) = \alpha \|\mathbf{W}\|_F^2 \text{ and } \psi(\mathbf{H}) = \beta \|\mathbf{H}\|_F^2. \tag{20}$$

279 The Frobenius-norm regularization may be used to prevent the elements of  $\mathbf{W}$  or  $\mathbf{H}$  from  
 280 growing too large in their absolute values. It can also be adopted to stabilize the BCD methods.  
 281 In the two matrix block case, since the uniqueness of the minimum of each subproblem is  
 282 not required according to Corollary 1,  $\mathbf{H}$  in (7a) or  $\mathbf{W}$  in (7b) need not be of full column  
 283 rank. The full column rank condition is however required for some algorithms for the NLS  
 284 subproblems, as discussed in Sect. 4. As shown below, the Frobenius-norm regularization  
 285 ensures that the NLS subproblems of the two matrix block case are always defined with  
 286 a matrix of full column rank. Similarly in the  $2K$  vector block or the  $K(M + N)$  scalar  
 287 block cases, the condition that  $\mathbf{w}_k$  and  $\mathbf{h}_k$  remain nonzero throughout all the iterations can  
 288 be relaxed when the Frobenius-norm regularization is used.

289 Applying the BCD framework with two matrix blocks to (19) with the regularization term  
 290 in (20),  $\mathbf{W}$  can be updated as

$$291 \quad \mathbf{W} \leftarrow \arg \min_{\mathbf{W} \geq 0} \left\| \begin{pmatrix} \mathbf{H} \\ \sqrt{\alpha} \mathbf{I}_K \end{pmatrix} \mathbf{W}^T - \begin{pmatrix} \mathbf{A}^T \\ \mathbf{0}_{K \times M} \end{pmatrix} \right\|_F^2, \quad (21)$$

292 where  $\mathbf{I}_K$  is a  $K \times K$  identity matrix and  $\mathbf{0}_{K \times M}$  is a  $K \times M$  matrix containing only zeros,  
 293 and  $\mathbf{H}$  can be updated with a similar reformulation. Clearly, if  $\alpha$  is nonzero,  $\begin{pmatrix} \mathbf{H} \\ \sqrt{\alpha} \mathbf{I}_K \end{pmatrix}$  in  
 294 (21) is of full column rank. Applying the BCD framework with  $2K$  vector blocks, a column  
 295 of  $\mathbf{W}$  is updated as

$$296 \quad \mathbf{w}_k \leftarrow \left[ \frac{(\mathbf{H}^T \mathbf{H})_{kk}}{(\mathbf{H}^T \mathbf{H})_{kk} + \alpha} \mathbf{w}_k + \frac{(\mathbf{A}\mathbf{H})_{\cdot k} - (\mathbf{W}\mathbf{H}^T \mathbf{H})_{\cdot k}}{(\mathbf{H}^T \mathbf{H})_{kk} + \alpha} \right]_+. \quad (22)$$

297 If  $\alpha$  is nonzero, the solution of (22) is uniquely defined without requiring  $\mathbf{h}_k$  to be a nonzero  
 298 vector.

299 The  $l_1$ -norm regularization can be adopted to promote sparsity in the factor matrices. In  
 300 many areas such as linear regression [80] and signal processing [16], it has been widely known  
 301 that the  $l_1$ -norm regularization promotes sparse solutions. In NMF, sparsity was shown to  
 302 improve the part-based interpretation [47] and the clustering ability [52,57]. When sparsity  
 303 is desired on matrix  $\mathbf{H}$ , the  $l_1$ -norm regularization can be set as

$$304 \quad \phi(\mathbf{W}) = \alpha \|\mathbf{W}\|_F^2 \quad \text{and} \quad \psi(\mathbf{H}) = \beta \sum_{n=1}^N \|\mathbf{h}_n\|_1^2, \quad (23)$$

305 where  $\mathbf{h}_n$  represents the  $n$ th row of  $\mathbf{H}$ . The  $l_1$ -norm term of  $\psi(\mathbf{H})$  in (23) promotes sparsity  
 306 on  $\mathbf{H}$  while the Frobenius norm term of  $\phi(\mathbf{W})$  is needed to prevent  $\mathbf{W}$  from growing too  
 307 large. Similarly, sparsity can be imposed on  $\mathbf{W}$  or on both  $\mathbf{W}$  and  $\mathbf{H}$ .

308 Applying the BCD framework with two matrix blocks to (19) with the regularization term  
 309 in (23),  $\mathbf{W}$  can be updated as (21), and  $\mathbf{H}$  can be updated as

$$310 \quad \mathbf{H} \leftarrow \arg \min_{\mathbf{H} \geq 0} \left\| \begin{pmatrix} \mathbf{W} \\ \sqrt{\beta} \mathbf{1}_{1 \times K} \end{pmatrix} \mathbf{H}^T - \begin{pmatrix} \mathbf{A} \\ \mathbf{0}_{1 \times N} \end{pmatrix} \right\|_F^2, \quad (24)$$

311 where  $\mathbf{1}_{1 \times K}$  is a row vector of length  $K$  containing only ones. Applying the BCD framework  
 312 with  $2K$  vector blocks, a column of  $\mathbf{W}$  is updated as (22), and a column of  $\mathbf{H}$  is updated as

$$313 \quad \mathbf{h}_k \leftarrow \left[ \mathbf{h}_k + \frac{(\mathbf{A}^T \mathbf{W})_{\cdot k} - \mathbf{H}((\mathbf{W}^T \mathbf{W})_{\cdot k} + \beta \mathbf{1}_K)}{(\mathbf{W}^T \mathbf{W})_{kk} + \beta} \right]_+. \quad (25)$$

314 Note that the  $l_1$ -norm term in (23) is written as the sum of the *squares* of the  $l_1$ -norm of  
 315 the columns of  $\mathbf{H}$ . Alternatively, we can impose the  $l_1$ -norm based regularization without  
 316 squaring: That is,

$$317 \quad \phi(\mathbf{W}) = \alpha \|\mathbf{W}\|_F^2 \quad \text{and} \quad \psi(\mathbf{H}) = \beta \sum_{n=1}^N \sum_{k=1}^K |h_{nk}|. \quad (26)$$

318 Although both (23) and (26) promote sparsity, the squared form in (23) is easier to handle  
 319 with the two matrix block case, as shown above. Applying the  $2K$ -vector BCD framework  
 320 on (19) with the regularization term in (26), the update for a column of  $\mathbf{h}$  is written as

$$321 \quad \mathbf{h}_k \leftarrow \left[ \mathbf{h}_k + \frac{(\mathbf{A}^T \mathbf{W})_{\cdot k} - (\mathbf{H} \mathbf{W}^T \mathbf{W})_{\cdot k} + \frac{1}{2} \beta \mathbf{1}_K}{(\mathbf{W}^T \mathbf{W})_{kk}} \right]_+.$$

322 For more information, see [19], Section 4.7.4 of [22], and Section 4.5 of [44]. When the  
 323 BCD framework with two matrix blocks is used with the regularization term in (26), a  
 324 custom algorithm for  $l_1$ -regularized least squares problem has to be involved: See, e.g., [30].

### 325 3 Acceleration and other approaches

#### 326 3.1 Accelerated methods

327 The BCD methods described so far have been very successful for the NMF computation.  
 328 In addition, several techniques to accelerate the methods have been proposed. Korattikara  
 329 et al. [62] proposed a subsampling strategy to improve the two matrix block (i.e., ANLS)  
 330 case. Their main idea is to start with a small factorization problem, which is obtained by  
 331 random subsampling, and gradually increase the size of subsamples. Under the assumption  
 332 of asymptotic normality, the decision whether to increase the size is made based on sta-  
 333 tistical hypothesis testing. Gillis and Glineur [38] proposed a multi-level approach, which  
 334 also gradually increases the problem size based on a multi-grid representation. The method  
 335 in [38] is applicable not only to the ANLS methods, but also to the HALS/RRI method and  
 336 the multiplicative updating method.

337 Hsieh and Dhillon proposed a greedy coordinate descent method [48]. Unlike the  
 338 HALS/RRI method, in which every element is updated exactly once per iteration, they selec-  
 339 tively choose the elements whose update will lead to the largest decrease of the objective  
 340 function. Although their method does not follow the BCD framework, they showed that every  
 341 limit point generated by their method is a stationary point. Gillis and Glineur also proposed  
 342 an acceleration scheme for the HALS/RRI and the multiplicative updating methods: Unlike  
 343 the standard versions, their approach repeats updating the elements of  $\mathbf{W}$  several times before  
 344 updating the elements of  $\mathbf{H}$  [37]. Noticeable improvements in the speed of convergence is  
 345 reported.

#### 346 3.2 Multiplicative updating rules

347 The multiplicative updating rule [67] is by far the most popular algorithm for NMF. Each  
 348 element is updated through *multiplications* as

$$349 \quad w_{mk} \leftarrow w_{mk} \frac{(\mathbf{A}\mathbf{H})_{mk}}{(\mathbf{W}\mathbf{H}^T \mathbf{H})_{mk}}, \quad h_{nk} \leftarrow h_{nk} \frac{(\mathbf{A}^T \mathbf{W})_{nk}}{(\mathbf{H}\mathbf{W}^T \mathbf{W})_{nk}}. \quad (27)$$

Since elements are updated in this multiplication form, the nonnegativity is always satisfied when  $\mathbf{A}$  is nonnegative. This algorithm can be contrasted with the HALS/RRI algorithm as follows. The element-wise gradient descent updates for (2) can be written as

$$w_{mk} \leftarrow w_{mk} + \lambda_{mk} \left[ (\mathbf{A}\mathbf{H})_{mk} - (\mathbf{W}\mathbf{H}^T\mathbf{H})_{mk} \right] \text{ and}$$

$$h_{nk} \leftarrow h_{nk} + \mu_{nk} \left[ (\mathbf{A}^T\mathbf{W})_{nk} - (\mathbf{H}\mathbf{W}^T\mathbf{W})_{nk} \right],$$

where  $\lambda_{mk}$  and  $\mu_{nk}$  represent step-lengths. The multiplicative updating rule is obtained by taking

$$\lambda_{mk} = \frac{w_{mk}}{(\mathbf{W}\mathbf{H}^T\mathbf{H})_{mk}} \text{ and } \mu_{nk} = \frac{h_{nk}}{(\mathbf{H}\mathbf{W}^T\mathbf{W})_{nk}}, \tag{28}$$

whereas the HALS/RRI algorithm interpreted as the BCD method with scalar blocks as in (18) is obtained by taking

$$\lambda_{mk} = \frac{1}{(\mathbf{H}^T\mathbf{H})_{kk}} \text{ and } \mu_{nk} = \frac{1}{(\mathbf{W}^T\mathbf{W})_{kk}}. \tag{29}$$

The step-lengths chosen in the multiplicative updating rule is conservative enough so that the result is always nonnegative. On the other hand, the step-lengths chosen in the HALS/RRI algorithm could potentially lead to a nonnegative value, and therefore the projection  $[\cdot]_+$  is needed. Although the convergence property of the BCD framework holds for the HALS/RRI algorithm as in Corollary 3, it does not hold for the multiplicative updating rule since the step-lengths in (28) does not achieve the optimal solution. In practice, the convergence of the HALS/RRI algorithm is much faster than that of the multiplicative updating.

Lee and Seung [67] showed that under the multiplicative updating rule, the objective function in (2) is non-increasing. However, it is unknown whether it converges to a stationary point. Gonzalez and Zhang demonstrated the difficulty [40], and the slow convergence of multiplicative updates has been further reported in [53,58,59,71]. To overcome this issue, Lin [70] proposed a modified update rule for which every limit point is stationary; note that, after this modification, the update rule becomes additive instead of multiplicative.

Since the values are updated only through multiplications, the elements of  $\mathbf{W}$  and  $\mathbf{H}$  obtained by the multiplicative updating rule typically remain nonzero. Hence, its solution matrices typically are denser than those from the BCD methods. The multiplicative updating rule breaks down if a zero value occurs to an element of the denominators in (27). To circumvent this difficulty, practical implementations often add a small number, such as  $10^{-16}$ , to each element of the denominators.

### 3.3 Alternating least squares method

In the two-block BCD method of Sect. 2.1, it is required to find a minimum of the nonnegativity-constrained least squares (NLS) subproblems in (7). Earlier, Berry et al. has proposed to approximately solve the NLS subproblems hoping to accelerate the algorithm [4]. In their alternating least squares (ALS) method, they solved the least squares problems ignoring the nonnegativity constraints, and then negative elements in the computed solution matrix are set to zeros. That is,  $\mathbf{W}$  and  $\mathbf{H}$  are updated as

387 
$$\mathbf{W}^T \leftarrow \left[ \left( \mathbf{H}^T \mathbf{H} \right)^{-1} \left( \mathbf{H}^T \mathbf{A}^T \right) \right]_+ \text{ and} \tag{30a}$$

388 
$$\mathbf{H}^T \leftarrow \left[ \left( \mathbf{W}^T \mathbf{W} \right)^{-1} \left( \mathbf{W}^T \mathbf{A} \right) \right]_+ . \tag{30b}$$

389 When  $\mathbf{H}^T \mathbf{H}$  or  $\mathbf{W}^T \mathbf{W}$  is rank-deficient, the Moore-Penrose pseudo-inverse may be used  
 390 instead of the inverse operator. Unfortunately, results from (30) are not the minimizers of  
 391 subproblems (7). Although each subproblem of the ALS method can be solved efficiently,  
 392 the convergence property in Corollary 1 is not applicable to the ALS method. In fact, the  
 393 ALS method does not necessarily decrease the objective function after each iteration [59].

394 It is interesting to note that the HALS/RRI method does not have this difficulty although  
 395 the same element-wise projection is used. In the HALS/RRI method, a subproblem in the  
 396 form of

397 
$$\min_{\mathbf{x} \geq 0} \left\| \mathbf{b} \mathbf{x}^T - \mathbf{C} \right\|_F^2 \tag{31}$$

398 with  $\mathbf{b} \in \mathbb{R}^M$  and  $\mathbf{C} \in \mathbb{R}^{M \times N}$  is solved with  $\mathbf{x} \leftarrow \left[ \frac{\mathbf{C}^T \mathbf{b}}{\mathbf{b}^T \mathbf{b}} \right]_+$ , which is the optimal solution of  
 399 (31) as shown in Theorem 2. On the other hand, in the ALS algorithm, a subproblem in the  
 400 form of

401 
$$\min_{\mathbf{x} \geq 0} \left\| \mathbf{B} \mathbf{x} - \mathbf{c} \right\|_2^2 \tag{32}$$

402 with  $\mathbf{B} \in \mathbb{R}^{M \times N}$  and  $\mathbf{c} \in \mathbb{R}^M$  is solved with  $\mathbf{x} \leftarrow \left[ \left( \mathbf{B}^T \mathbf{B} \right)^{-1} \mathbf{B}^T \mathbf{c} \right]_+$ , which is not an optimal  
 403 solution of (32).

### 404 3.4 Successive rank one deflation

405 Some algorithms have been designed to compute NMF based on successive rank-one defla-  
 406 tion. This approach is motivated from the fact that the singular value decomposition (SVD)  
 407 can be computed through successive rank-one deflation. When considered for NMF, however,  
 408 the rank-one deflation method has a few issues as we summarize below.

409 Let us first recapitulate the deflation approach for SVD. Consider a matrix  $\mathbf{A} \in \mathbb{R}^{M \times N}$  of  
 410 rank  $R$ , and suppose its SVD is written as

411 
$$\mathbf{A} = \mathbf{U} \mathbf{\Sigma} \mathbf{V}^T = \sum_{r=1}^R \sigma_r \mathbf{u}_r \mathbf{v}_r^T, \tag{33}$$

412 where  $\mathbf{U} = [\mathbf{u}_1 \dots \mathbf{u}_R] \in \mathbb{R}^{M \times R}$  and  $\mathbf{V} = [\mathbf{v}_1 \dots \mathbf{v}_R] \in \mathbb{R}^{N \times R}$  are orthogonal matrices,  
 413 and  $\mathbf{\Sigma} \in \mathbb{R}^{R \times R}$  is a diagonal matrix having  $\sigma_1 \geq \dots \geq \sigma_R \geq 0$  in the diagonal. The rank- $K$   
 414 SVD for  $K < R$  is obtained by taking only the first  $K$  singular values and corresponding  
 415 singular vectors:

416 
$$\tilde{\mathbf{A}}_K = \tilde{\mathbf{U}}_K \tilde{\mathbf{\Sigma}}_K \tilde{\mathbf{V}}_K^T = \sum_{k=1}^K \sigma_k \mathbf{u}_k \mathbf{v}_k^T,$$

417 where  $\tilde{\mathbf{U}}_K \in \mathbb{R}^{M \times K}$  and  $\tilde{\mathbf{V}}_K \in \mathbb{R}^{N \times K}$  are sub-matrices of  $\mathbf{U}$  and  $\mathbf{V}$  obtained by taking the  
 418 leftmost  $K$  columns. It is well-known that the best rank- $K$  approximation of  $\mathbf{A}$  in terms of  
 419 minimizing the  $l_2$ -norm or the Frobenius norm of the residual matrix is the rank- $K$  SVD: See  
 420 Theorem 2.5.3 in Page 72 of Golub and Van Loan [39]. The rank- $K$  SVD can be computed

421 through successive rank one deflation as follows. First, the best rank-one approximation,  
 422  $\sigma_1 \mathbf{u}_1 \mathbf{v}_1^T$ , is computed with an efficient algorithm such as the power iteration. Then, the  
 423 residual matrix is obtained as  $\tilde{\mathbf{E}}_1 = \mathbf{A} - \sigma_1 \mathbf{u}_1 \mathbf{v}_1^T = \sum_{r=2}^R \sigma_r \mathbf{u}_r \mathbf{v}_r^T$ , and the rank of  $\tilde{\mathbf{E}}_1$  is  
 424  $R - 1$ . For the residual matrix  $\tilde{\mathbf{E}}_1$ , its best rank-one approximation,  $\sigma_2 \mathbf{u}_2 \mathbf{v}_2^T$ , is obtained,  
 425 and the residual matrix  $\tilde{\mathbf{E}}_2$ , whose rank is  $R - 2$ , can be found in the same manner:  $\tilde{\mathbf{E}}_2 =$   
 426  $\tilde{\mathbf{E}}_1 - \sigma_2 \mathbf{u}_2 \mathbf{v}_2^T = \sum_{r=3}^R \sigma_r \mathbf{u}_r \mathbf{v}_r^T$ . Repeating this process for  $K$  times, one can obtain the rank- $K$   
 427 SVD.

428 When it comes to NMF, a notable theoretical result about nonnegative matrices relates  
 429 SVD and NMF when  $K = 1$ . The following theorem, which extends the Perron-Frobenius  
 430 theorem [3,45], is shown in Chapter 2 of Berman and Plemmons [3].

431 **Theorem 3** For a nonnegative symmetric matrix  $\mathbf{A} \in \mathbb{R}_+^{N \times N}$ , the eigenvalue of  $\mathbf{A}$  with the  
 432 largest magnitude is nonnegative, and there exists a nonnegative eigenvector corresponding  
 433 to the largest eigenvalue.

434 A direct consequence of Theorem 3 is the nonnegativity of the best rank-one approxima-  
 435 tion.

436 **Corollary 4** (Nonnegativity of best rank-one approximation) For any nonnegative matrix  
 437  $\mathbf{A} \in \mathbb{R}_+^{M \times N}$ , the following minimization problem

438 
$$\min_{\mathbf{u} \in \mathbb{R}^M, \mathbf{v} \in \mathbb{R}^N} \|\mathbf{A} - \mathbf{u}\mathbf{v}^T\|_F^2. \tag{34}$$

439 has an optimal solution satisfying  $\mathbf{u} \geq 0$  and  $\mathbf{v} \geq 0$ .

440 Another way to realizing Corollary 4 is through the use of the SVD. For a nonnegative  
 441 matrix  $\mathbf{A} \in \mathbb{R}_+^{M \times N}$  and for any vectors  $\mathbf{u} \in \mathbb{R}^M$  and  $\mathbf{v} \in \mathbb{R}^N$ ,

442 
$$\begin{aligned} \|\mathbf{A} - \mathbf{u}\mathbf{v}^T\|_F^2 &= \sum_{m=1}^M \sum_{n=1}^N (a_{mn} - u_m v_n)^2 \\ &\geq \sum_{m=1}^M \sum_{n=1}^N (a_{mn} - |u_m| |v_n|)^2. \end{aligned} \tag{35}$$

443

444 Hence, element-wise absolute values can be taken from the left and right singular vectors that  
 445 correspond to the largest singular value to achieve the best rank-one approximation satisfying  
 446 nonnegativity. There might be other optimal solutions of (34) involving negative numbers:  
 447 See [34].

448 The elegant property in Corollary 4, however, is not readily applicable when  $K \geq 2$ . After  
 449 the best rank-one approximation matrix is deflated, the residual matrix may contain negative  
 450 elements, and then Corollary 4 is not applicable any more. In general, successive rank-one  
 451 deflation is not an optimal approach for NMF computation. Let us take a look at a small  
 452 example which demonstrates this issue. Consider matrix  $\mathbf{A}$  given as

453 
$$\mathbf{A} = \begin{pmatrix} 4 & 6 & 0 \\ 6 & 4 & 0 \\ 0 & 0 & 1 \end{pmatrix}.$$

454 The best rank-one approximation of  $\mathbf{A}$  is shown as  $\mathbf{A}_1$  below. The residual is  $\mathbf{E}_1 = \mathbf{A} - \mathbf{A}_1$ ,  
 455 which contains negative elements:

$$\mathbf{A}_1 = \begin{pmatrix} 5 & 5 & 0 \\ 5 & 5 & 0 \\ 0 & 0 & 0 \end{pmatrix}, \mathbf{E}_1 = \begin{pmatrix} -1 & 1 & 0 \\ 1 & -1 & 0 \\ 0 & 0 & 1 \end{pmatrix}.$$

One of the best rank-one approximations of  $\mathbf{E}_1$  with nonnegativity constraints is  $\mathbf{A}_2$ , and the residual matrix is  $\mathbf{E}_2 = \mathbf{A}_1 - \mathbf{A}_2$ :

$$\mathbf{A}_2 = \begin{pmatrix} 0 & 0 & 0 \\ 0 & 0 & 0 \\ 0 & 0 & 1 \end{pmatrix}, \mathbf{E}_2 = \begin{pmatrix} -1 & 1 & 0 \\ 1 & -1 & 0 \\ 0 & 0 & 0 \end{pmatrix}.$$

The nonnegative rank-two approximation obtained by this rank-one deflation approach is

$$\mathbf{A}_1 + \mathbf{A}_2 = \begin{pmatrix} 5 & 5 & 0 \\ 5 & 5 & 0 \\ 0 & 0 & 1 \end{pmatrix}.$$

However, the best nonnegative rank-two approximation of  $\mathbf{A}$  is in fact  $\hat{\mathbf{A}}_2$  with residual matrix  $\hat{\mathbf{E}}_2$ :

$$\hat{\mathbf{A}}_2 = \begin{pmatrix} 4 & 6 & 0 \\ 6 & 4 & 0 \\ 0 & 0 & 0 \end{pmatrix}, \hat{\mathbf{E}}_2 = \begin{pmatrix} 0 & 0 & 0 \\ 0 & 0 & 0 \\ 0 & 0 & 1 \end{pmatrix}.$$

Therefore, a strategy that successively finds the best rank-one approximation with nonnegativity constraints and deflates in each step does not necessarily lead to an optimal solution of NMF.

Due to this difficulty, some variations of rank-one deflation have been investigated for NMF. Biggs et al. [6] proposed a rank-one reduction algorithm in which they look for a nonnegative submatrix that is close to a rank-one approximation. Once such a submatrix is identified, they compute the best rank-one approximation using the power method and ignore the residual. Gillis and Glineur [36] sought a nonnegative rank-one approximation under the constraint that the residual matrix remains element-wise nonnegative. Due to the constraints, however, the problem of finding the nonnegative rank-one approximation becomes more complicated and computationally expensive than the power iteration. Optimization properties such as a convergence to a stationary point has not been shown for these modified rank-one reduction methods.

It is worth noting the difference between the HALS/RRI algorithm, described as the  $2K$  vector block case in Sect. 2.2, and the rank-one deflation method. These approaches are similar in that the rank-one approximation problem with nonnegativity constraints is solved in each step, filling in the  $k$ th columns of  $\mathbf{W}$  and  $\mathbf{H}$  with the solution for  $k = 1, \dots, K$ . In the rank-one deflation method, once the  $k$ th columns of  $\mathbf{W}$  and  $\mathbf{H}$  are computed, they are fixed and kept as a part of the final solution before the  $(k + 1)$ th columns are computed. On the other hand, the HALS/RRI algorithm updates all the columns through multiple iterations until a local minimum is achieved. This simultaneous searching for all  $2K$  vectors throughout the iterations is necessary to achieve an optimal solution of NMF, unlike in the case of SVD.

#### 4 Algorithms for the nonnegativity constrained least squares problems

We review numerical methods developed for the NLS subproblems in (7). For simplicity, we consider the following notations in this section:

$$\min_{\mathbf{X} \geq 0} \|\mathbf{B}\mathbf{X} - \mathbf{C}\|_F^2 = \sum_{r=1}^R \|\mathbf{B}\mathbf{x}_r - \mathbf{c}_r\|_2^2, \tag{36}$$

where  $\mathbf{B} \in \mathbb{R}^{P \times Q}$ ,  $\mathbf{C} = [\mathbf{c}_1, \dots, \mathbf{c}_R] \in \mathbb{R}^{Q \times R}$ , and  $\mathbf{X} = [\mathbf{x}_1, \dots, \mathbf{x}_R] \in \mathbb{R}^{Q \times R}$ . We mainly discuss two groups of algorithms for the NLS problems. The first group consists of the gradient descent and the Newton-type methods that are modified to satisfy the nonnegativity constraints using a projection operator. The second group consists of the active-set and the active-set-like methods, in which zero and nonzero variables are explicitly kept track of and a system of linear equations is solved at each iteration. For more details, see Lawson and Hanson [64], Bjork [8], and Chen and Plemmons [15].

To facilitate our discussion, we state a simple NLS problem with a single right-hand side:

$$\min_{\mathbf{x} \geq 0} g(\mathbf{x}) = \|\mathbf{B}\mathbf{x} - \mathbf{c}\|_2^2. \tag{37}$$

Problem (36) may be solved by handling independent problems for the columns of  $\mathbf{X}$ , whose form appears as (37). Otherwise, the problem in (36) can also be transformed into

$$\min_{\mathbf{x}_1, \dots, \mathbf{x}_R \geq 0} \left\| \begin{pmatrix} \mathbf{B} & & \\ & \ddots & \\ & & \mathbf{B} \end{pmatrix} \begin{pmatrix} \mathbf{x}_1 \\ \vdots \\ \mathbf{x}_R \end{pmatrix} - \begin{pmatrix} \mathbf{c}_1 \\ \vdots \\ \mathbf{c}_R \end{pmatrix} \right\|_2^2. \tag{38}$$

#### 4.1 Projected iterative methods

Projected iterative methods for the NLS problems are designed based on the fact that the objective function in (36) is differentiable and that the projection to the nonnegative orthant is easy to compute. The first method of this type proposed for NMF was the projected gradient method of Lin [71]. Their update formula is written as

$$\mathbf{x}^{(i+1)} \leftarrow \left[ \mathbf{x}^{(i)} - \alpha^{(i)} \nabla g(\mathbf{x}^{(i)}) \right]_+, \tag{39}$$

where  $\mathbf{x}^{(i)}$  and  $\alpha^{(i)}$  represent the variables and the step length at the  $i$ th iteration. Step length  $\alpha^{(i)}$  is chosen by a back-tracking line search to satisfy Armijo’s rule with an optional stage that increases the step length. Kim et al. [51] proposed a quasi-Newton method by utilizing the second order information to improve convergence:

$$\mathbf{x}^{(i+1)} \leftarrow \left( \left[ \mathbf{y}^{(i)} - \alpha^{(i)} \mathbf{D}^{(i)} \nabla g(\mathbf{y}^{(i)}) \right]_+ \right), \tag{40}$$

where  $\mathbf{y}^{(i)}$  is a subvector of  $\mathbf{x}^{(i)}$  with elements that are not optimal in terms of the Karush–Kuhn–Tucker (KKT) conditions. They efficiently updated  $\mathbf{D}^{(i)}$  using the BFGS method and selected  $\alpha^{(i)}$  by a back-tracking line search. Whereas Lin considered a stacked-up problem as in (38), the quasi-Newton method by Kim et al. was applied to each column separately.

A notable variant of the projected gradient method is the Barzilai-Borwein method [7]. Han et al. [42] proposed alternating projected Barzilai-Borwein method for NMF. A key characteristic of the Barzilai-Borwein method in unconstrained quadratic programming is that the step-length is chosen by a closed-form formula without having to perform a line search:

$$\mathbf{x}^{(i+1)} \leftarrow \left[ \mathbf{x}^{(i)} - \alpha^{(i)} \nabla g(\mathbf{x}^{(i)}) \right]_+ \text{ with } \alpha^{(i)} = \frac{\mathbf{s}^T \mathbf{s}}{\mathbf{y}^T \mathbf{s}}, \text{ where}$$

$$\mathbf{s} = \mathbf{x}^{(i)} - \mathbf{x}^{(i-1)} \text{ and } \mathbf{y} = \nabla g(\mathbf{x}^{(i)}) - \nabla g(\mathbf{x}^{(i-1)}).$$

---

**Algorithm 1** Outline of the Active-set Method for  $\min_{\mathbf{x} \geq 0} g(\mathbf{x}) = \|\mathbf{B}\mathbf{x} - \mathbf{c}\|_2^2$  (See [64] for more details)

---

- 1: Initialize  $\mathbf{x}$  (typically with all zeros).
- 2: Set  $\mathcal{I}, \mathcal{E}$  (working sets) to be indices representing zero and nonzero variables. Let  $\mathbf{x}_{\mathcal{I}}$  and  $\mathbf{x}_{\mathcal{E}}$  denote the subvectors of  $\mathbf{x}$  with corresponding indices, and let  $\mathbf{B}_{\mathcal{I}}$  and  $\mathbf{B}_{\mathcal{E}}$  denote the submatrices of  $\mathbf{B}$  with corresponding column indices.
- 3: **for**  $i = 1, 2, \dots$  **do**
- 4:   Solve an unconstrained least squares problem,

$$\min_{\mathbf{z}} \|\mathbf{B}_{\mathcal{E}}\mathbf{z} - \mathbf{c}\|_2^2. \quad (41)$$

- 5:   Check if the solution is nonnegative and satisfies KKT conditions. If so, set  $\mathbf{x}_{\mathcal{E}} \leftarrow \mathbf{z}$ , set  $\mathbf{x}_{\mathcal{I}}$  with zeros, and return  $\mathbf{x}$  as a solution. Otherwise, update  $\mathbf{x}, \mathcal{I}$ , and  $\mathcal{E}$ .
  - 6: **end for**
- 

525 When the nonnegativity constraints are given, however, back-tracking line search still had to  
 526 be employed. Han et al. discussed a few variations of the Barzilai-Borwein method for NMF  
 527 and reported that the algorithms outperform Lin's method.

528 Many other methods have been developed. Merritt and Zhang [73] proposed an interior  
 529 point gradient method, and Friedlander and Hatz [32] used a two-metric projected gradient  
 530 method in their study on NTF. Zdunek and Cichocki [86] proposed a quasi-Newton method,  
 531 but its lack of convergence was pointed out [51]. Zdunek and Cichocki [87] also studied the  
 532 projected Landweber method and the projected sequential subspace method.

#### 533 4.2 Active-set and active-set-like methods

534 The active-set method for the NLS problems is due to Lawson and Hanson [64]. A key  
 535 observation is that, if the zero and nonzero elements of the final solution are known in  
 536 advance, the solution can be easily computed by solving an unconstrained least squares  
 537 problem for the nonzero variables and setting the rest to zeros. The sets of zero and nonzero  
 538 variables are referred to as *active* and *passive* sets, respectively. In the active-set method,  
 539 so-called *workings sets* are kept track of until the optimal active and passive sets are found.  
 540 A rough pseudo-code for the active-set method is shown in Algorithm 1.

541 Lawson and Hanson's method has been a standard for the NLS problems, but applying  
 542 it directly to NMF is very slow. When used for NMF, it can be accelerated in two differ-  
 543 ent ways. The first approach is to use the QR decomposition to solve (41) or the Cholesky  
 544 decomposition to solve the normal equations  $(\mathbf{B}_{\mathcal{E}}^T \mathbf{B}_{\mathcal{E}}) \mathbf{z} = \mathbf{B}_{\mathcal{E}}^T \mathbf{c}$  and have the Cholesky or  
 545 QR factors updated by the Givens rotations [39]. The second approach, which was proposed  
 546 by Bro and De Jong [9] and Ven Benthem and Keenan [81], is to identify common compu-  
 547 tations in solving the NLS problems with multiple right-hand sides. More information and  
 548 experimental comparisons of these two approaches are provided in [59].

549 The active-set methods possess a property that the objective function decreases after each  
 550 iteration; however, maintaining this property often limits its scalability. A main computational  
 551 burden of the active-set methods is in solving the unconstrained least squares problem (41);  
 552 hence, the number of iterations required until termination considerably affects the computa-  
 553 tion cost. In order to achieve the monotonic decreasing property, typically only one variable  
 554 is exchanged between working sets per iteration. As a result, when the number of unknowns  
 555 is large, the number of iterations required for termination grows, slowing down the method.  
 556 The block principal pivoting method developed by Kim and Park [58,59] overcomes this

557 limitation. Their method, which is based on the work of Judice and Pires [50], allows the  
558 exchanges of multiple variables between working sets. This method does not maintain the  
559 nonnegativity of intermediate vectors nor the monotonic decrease of the objective function,  
560 but it requires a smaller number of iterations until termination than the active set methods. It  
561 is worth emphasizing that the grouping-based speed-up technique, which was earlier devised  
562 for the active-set method, is also effective with the block principal pivoting method for the  
563 NMF computation: For more details, see [59].

#### 564 4.3 Discussion and other methods

565 A main difference between the projected iterative methods and the active-set-like methods  
566 for the NLS problems lies in their convergence or termination. In projected iterative methods,  
567 a sequence of tentative solutions is generated so that an optimal solution is approached in  
568 the limit. In practice, one has to somehow stop iterations and return the current estimate,  
569 which might be only an approximation of the solution. In the active-set and active-set-like  
570 methods, in contrast, there is no concept of a limit point. Tentative solutions are generated  
571 with a goal of finding the optimal active and passive set partitioning, which is guaranteed  
572 to be found in a finite number of iterations since there are only a finite number of possible  
573 active and passive set partitionings. Once the optimal active and passive sets are found,  
574 the methods terminate. There are trade-offs of these behavior. While the projected iterative  
575 methods may return an approximate solution after a few number of iterations, the active-set  
576 and active-set-like methods only return a solution after they terminate. After the termination,  
577 however, the solution from the active-set-like methods is an exact solution only subject to  
578 numerical rounding errors while the solution from the projected iterative methods might be  
579 an approximate one.

580 Other approaches for solving the NLS problems can be considered as a subroutine for the  
581 NMF computation. Bellavia et al. [2] have studied an interior point Newton-like method, and  
582 Franc et al. [31] presented a sequential coordinate-wise method. Some observations about the  
583 NMF computation based on these methods as well as other methods are offered in Cichocki  
584 et al. [22]. Chu and Lin [18] proposed an algorithm based on low-dimensional polytope  
585 approximation: Their algorithm is motivated by a geometrical interpretation of NMF that  
586 data points are approximated by a simplicial cone [27].

587 Different conditions are required for the NLS algorithms to guarantee convergence or  
588 termination. The requirement of the projected gradient method [71] is mild as it only requires  
589 an appropriate selection of the step-length. Both the quasi-Newton method [51] and the  
590 interior point gradient method [73] require that matrix  $\mathbf{B}$  in (37) is of full column rank. The  
591 active-set method [53,64] does not require the full-rank condition as long as a zero vector is  
592 used for initialization [28]. In the block principal pivoting method [58,59], on the other hand,  
593 the full-rank condition is required. Since NMF is formulated as a lower rank approximation  
594 and  $K$  is typically much smaller than the rank of the input matrix, the ranks of both  $\mathbf{W}$  and  $\mathbf{H}$  in  
595 (7) typically remain full. When this condition is not likely to be satisfied, the Frobenius-norm  
596 regularization of Sect. 2.4 can be adopted to guarantee the full rank condition.

### 597 5 BCD framework for nonnegative CP

598 Our discussion on the low-rank factorizations of nonnegative matrices naturally extends  
599 to those of nonnegative tensors. In this section, we discuss nonnegative CANDE-  
600 COMP/PARAFAC (NCP) and explain how it can be computed by the BCD framework.

601 A few other decomposition models of higher order tensors have been studied, and interested  
 602 readers are referred to [1, 61]. The organization of this section is similar to that of Sect. 2,  
 603 and we will show that the NLS algorithms reviewed in Sect. 4 can also be used to factorize  
 604 tensors.

605 Let us consider an  $N$ th-order tensor  $\mathcal{A} \in \mathbb{R}^{M_1 \times \dots \times M_N}$ . For an integer  $K$ , we are  
 606 interested in finding nonnegative factor matrices  $\mathbf{H}^{(1)}, \dots, \mathbf{H}^{(N)}$  where  $\mathbf{H}^{(n)} \in \mathbb{R}^{M_n \times K}$  for  
 607  $n = 1, \dots, N$  such that

$$608 \quad \mathcal{A} \approx \llbracket \mathbf{H}^{(1)}, \dots, \mathbf{H}^{(N)} \rrbracket, \tag{42}$$

610 where

$$611 \quad \mathbf{H}^{(n)} = \left[ \mathbf{h}_1^{(n)} \dots \mathbf{h}_K^{(n)} \right] \text{ for } n = 1, \dots, N \text{ and} \tag{43}$$

$$612 \quad \llbracket \mathbf{H}^{(1)}, \dots, \mathbf{H}^{(N)} \rrbracket = \sum_{k=1}^K \mathbf{h}_k^{(1)} \circ \dots \circ \mathbf{h}_k^{(N)}. \tag{44}$$

616 The ‘ $\circ$ ’ symbol represents the outer product of vectors, and a tensor in the form of  
 617  $\mathbf{h}_k^{(1)} \circ \dots \circ \mathbf{h}_k^{(N)}$  is called a *rank-one* tensor. Model (42) is known as CANDECOMP/PARAFAC  
 618 (CP) [14, 43]: In the CP decomposition,  $\mathcal{A}$  is represented as the sum of  $K$  rank-one tensors.  
 619 The smallest integer  $K$  for which (42) holds as equality is called the *rank* of tensor  $\mathcal{A}$ . The  
 620 CP decomposition reduces to a matrix decomposition if  $N = 2$ . The nonnegative CP decom-  
 621 position is obtained by adding nonnegativity constraints to factor matrices  $\mathbf{H}^{(1)}, \dots, \mathbf{H}^{(N)}$ .  
 622 A corresponding problem can be written as, for  $\mathcal{A} \in \mathbb{R}_+^{M_1 \times \dots \times M_N}$ ,

$$623 \quad \min_{\mathbf{H}^{(1)}, \dots, \mathbf{H}^{(N)}} f(\mathbf{H}^{(1)}, \dots, \mathbf{H}^{(N)}) = \left\| \mathcal{A} - \llbracket \mathbf{H}^{(1)}, \dots, \mathbf{H}^{(N)} \rrbracket \right\|_F^2,$$

$$624 \quad \text{s.t. } \mathbf{H}^{(n)} \geq 0 \text{ for } n = 1, \dots, N. \tag{45}$$

627 We discuss algorithms for solving (45) in this section [19, 32, 54, 60]. Toward that end, we  
 628 introduce definitions of some operations of tensors.

629 **Mode- $n$  matricization:** The mode- $n$  matricization of  $\mathcal{A} \in \mathbb{R}^{M_1 \times \dots \times M_N}$ , denoted by  $\mathbf{A}^{<n>}$ ,  
 630 is a matrix obtained by linearizing all the indices of tensor  $\mathcal{A}$  except  $n$ . Specifically,  $\mathbf{A}^{<n>}$  is  
 631 a matrix of size  $M_n \times (\prod_{\tilde{n}=1, \tilde{n} \neq n}^N M_{\tilde{n}})$ , and the  $(m_1, \dots, m_N)$ th element of  $\mathcal{A}$  is mapped to  
 632 the  $(m_n, J)$ th element of  $\mathbf{A}^{<n>}$  where

$$633 \quad J = 1 + \sum_{j=1}^N (m_j - 1)J_j \text{ and } J_j = \prod_{l=1, l \neq n}^{j-1} M_l.$$

634 **Mode- $n$  fibers:** The fibers of higher-order tensors are vectors obtained by specifying  
 635 all indices except one. Given a tensor  $\mathcal{A} \in \mathbb{R}^{M_1 \times \dots \times M_N}$ , a mode- $n$  fiber denoted by  
 636  $\mathbf{a}_{m_1 \dots m_{n-1} : m_{n+1} \dots m_N}$  is a vector of length  $M_n$  with all the elements having  $m_1, \dots, m_{n-1}$ ,  
 637  $m_{n+1}, \dots, m_N$  as indices for the 1st,  $\dots$ ,  $(n-1)$ th,  $(n+2)$ th,  $\dots$ ,  $N$ th orders. The columns  
 638 and the rows of a matrix are the mode-1 and the mode-2 fibers, respectively.

639 **Mode- $n$  product:** The mode- $n$  product of a tensor  $\mathcal{A} \in \mathbb{R}^{M_1 \times \dots \times M_N}$  and a matrix  $\mathbf{U} \in$   
 640  $\mathbb{R}^{J \times M_n}$ , denoted by  $\mathcal{A} \times_n \mathbf{U}$ , is a tensor obtained by multiplying all mode- $n$  fibers of  $\mathcal{A}$  with  
 641 the columns of  $\mathbf{U}$ . The result is a tensor of size  $M_1 \times \dots \times M_{n-1} \times J \times M_{n+1} \times \dots \times M_N$   
 642 having elements as

$$643 \quad (\mathcal{A} \times_n \mathbf{U})_{m_1 \dots m_{n-1} j m_{n+1} \dots m_N} = \sum_{m_n=1}^{M_n} x_{m_1 \dots m_N} u_{j m_n}.$$

644 In particular, the mode- $n$  product of  $\mathcal{A}$  and a vector  $\mathbf{u} \in \mathbb{R}^{M_n}$  is a tensor of size  $M_1 \times \cdots \times$   
 645  $M_{n-1} \times M_{n+1} \times \cdots \times M_N$ .  
 646 **Khatri-Rao product:** The Khatri-Rao product of two matrices  $\mathbf{A} \in \mathbb{R}^{J_1 \times L}$  and  $\mathbf{B} \in \mathbb{R}^{J_2 \times L}$ ,  
 647 denoted by  $\mathbf{A} \odot \mathbf{B} \in \mathbb{R}^{(J_1 J_2) \times L}$ , is defined as

$$648 \quad \mathbf{A} \odot \mathbf{B} = \begin{bmatrix} a_{11}\mathbf{b}_1 & a_{12}\mathbf{b}_2 & \cdots & a_{1L}\mathbf{b}_L \\ a_{21}\mathbf{b}_1 & a_{22}\mathbf{b}_2 & \cdots & a_{2L}\mathbf{b}_L \\ \vdots & \vdots & \ddots & \vdots \\ a_{J_1 1}\mathbf{b}_1 & a_{J_1 2}\mathbf{b}_2 & \cdots & a_{J_1 L}\mathbf{b}_L \end{bmatrix}.$$

649 5.1 BCD with  $N$  matrix blocks

650 A simple BCD method can be designed for (45) considering each of the factor matrices  
 651  $\mathbf{H}^{(1)}, \dots, \mathbf{H}^{(N)}$  as a block. Using notations introduced above, approximation model (42) can  
 652 be written as, for any  $n \in \{1, \dots, N\}$ ,

$$653 \quad \mathbf{A}^{<n>} \approx \mathbf{H}^{(n)} \left( \mathbf{B}^{(n)} \right)^T, \tag{46}$$

654 where

$$655 \quad \mathbf{B}^{(n)} = \mathbf{H}^{(N)} \odot \cdots \odot \mathbf{H}^{(n+1)} \odot \mathbf{H}^{(n-1)} \odot \cdots \odot \mathbf{H}^{(1)}$$

$$656 \quad \in \mathbb{R}^{(\prod_{\tilde{n}=1, \tilde{n} \neq n}^N M_{\tilde{n}}) \times K}.$$

657 Representation in (46) simplifies the treatment of this  $N$  matrix block case. After  
 658  $\mathbf{H}^{(2)}, \dots, \mathbf{H}^{(N)}$  are initialized with nonnegative elements, the following subproblem is solved  
 659 iteratively for  $n = 1, \dots, N$ :

$$663 \quad \mathbf{H}^{(n)} \leftarrow \arg \min_{\mathbf{H} \geq 0} \left\| \mathbf{B}^{(n)} \mathbf{H}^T - (\mathbf{A}^{<n>})^T \right\|_F^2. \tag{48}$$

664 Since subproblem (48) is an NLS problem, as in the matrix factorization case, this matrix-  
 665 block BCD method is called the alternating nonnegative least squares (ANLS) framework  
 666 [32, 54, 60]. The convergence property of the BCD method in Theorem 1 yields the following  
 667 corollary.

668 **Corollary 5** *If a unique solution exists for (48) and is attained for  $n = 1, \dots, N$ , then every*  
 669 *limit point of the sequence  $\left\{ (\mathbf{H}^{(1)}, \dots, \mathbf{H}^{(N)})^{(i)} \right\}$  generated by the ANLS framework is a*  
 670 *stationary point of (45).*

671 In particular, if each  $\mathbf{B}^{(n)}$  is of full column rank, the subproblem has a unique solution.  
 672 Algorithms for the NLS subproblems discussed in Sect. 4 can be used to solve (48).

673 For higher order tensors, the number of rows in  $\mathbf{B}^{(n)}$  and  $(\mathbf{A}^{<n>})^T$ , i.e.,  $\prod_{\tilde{n}=1, \tilde{n} \neq n}^N M_{\tilde{n}}$ , can  
 674 be quite large. However, often  $\mathbf{B}^{(n)}$  and  $(\mathbf{A}^{<n>})^T$  do not need to be explicitly constructed. In  
 675 most algorithms explained in Sect. 4, it is enough to have  $\mathbf{B}^{(n)T} (\mathbf{A}^{<n>})^T$  and  $(\mathbf{B}^{(n)})^T \mathbf{B}^{(n)}$ .  
 676 It is easy to verify that  $\mathbf{B}^{(n)T} (\mathbf{A}^{<n>})^T$  can be obtained by successive mode- $n$  products:

$$678 \quad \mathbf{B}^{(n)T} (\mathbf{A}^{<n>})^T = \mathcal{A} \times_1 \mathbf{H}^{(1)} \cdots \times_{(n-1)} \mathbf{H}^{(n-1)}$$

$$679 \quad \times_{(n)} \mathbf{H}^{(n)} \cdots \times_{(N)} \mathbf{H}^{(N)}. \tag{49}$$

682 In addition,  $(\mathbf{B}^{(n)})^T \mathbf{B}^{(n)}$  can be obtained as

$$683 \quad (\mathbf{B}^{(n)})^T \mathbf{B}^{(n)} = \bigotimes_{\tilde{n}=1, \tilde{n} \neq n}^N (\mathbf{H}^{(\tilde{n})})^T \mathbf{H}^{(\tilde{n})}, \quad (50)$$

684 where  $\otimes$  represents element-wise multiplication.

686 5.2 BCD with  $KN$  vector blocks

687 Another way to apply the BCD framework to (45) is to treat each column of  $\mathbf{H}^{(1)}, \dots, \mathbf{H}^{(N)}$   
 688 as a block. The columns are updated by solving, for  $n = 1, \dots, N$  and for  $k = 1, \dots, K$ ,

$$689 \quad \mathbf{h}_k^{(n)} \leftarrow \arg \min_{\mathbf{h} \geq 0} \left\| \llbracket \mathbf{h}_k^{(1)}, \dots, \mathbf{h}_k^{(n-1)}, \mathbf{h}, \mathbf{h}_k^{(n+1)}, \dots, \mathbf{h}_k^{(N)} \rrbracket - \mathcal{R}_k \right\|_F^2. \quad (51)$$

693 where

$$694 \quad \mathcal{R}_k = \mathcal{A} - \sum_{\tilde{k}=1, \tilde{k} \neq k}^K \mathbf{h}_{\tilde{k}}^{(1)} \circ \dots \circ \mathbf{h}_{\tilde{k}}^{(N)}.$$

695 Using matrix notations, problem (51) can be rewritten as

$$696 \quad \mathbf{h}_k^{(n)} \leftarrow \arg \min_{\mathbf{h} \geq 0} \left\| \mathbf{b}_k^{(n)} \mathbf{h}^T - (\mathbf{R}_k^{<n>})^T \right\|_F^2, \quad (52)$$

698 where  $\mathbf{R}_k^{<n>}$  is the mode- $n$  matricization of  $\mathcal{R}_k$  and

$$699 \quad \mathbf{b}_k^{(n)} = \mathbf{h}_k^{(N)} \circ \dots \circ \mathbf{h}_k^{(n+1)} \circ \mathbf{h}_k^{(n-1)} \circ \dots \circ \mathbf{h}_k^{(1)} \\ 700 \quad \in \mathbb{R}^{\left(\prod_{\tilde{n}=1, \tilde{n} \neq n}^N M_{\tilde{n}}\right) \times 1}. \quad (53)$$

703 This vector-block BCD method corresponds to the HALS method by Cichocki et al. for  
 704 NTF [19,22]. The convergence property in Theorem 1 yields the following corollary.

705 **Corollary 6** *If a unique solution exists for (52) and is attained for  $n = 1, \dots, N$  and for*  
 706  *$k = 1, \dots, K$ , every limit point of the sequence  $\left\{ (\mathbf{H}^{(1)}, \dots, \mathbf{H}^{(N)})^{(i)} \right\}$  generated by the*  
 707 *vector-block BCD method is a stationary point of (45).*

708 Using Theorem 2, the solution of (52) is

$$709 \quad \mathbf{h}_k^{(n)} \leftarrow \frac{\left[ \mathbf{R}_k^{<n>} \mathbf{b}_k^{(n)} \right]_+}{\left\| \mathbf{b}_k^{(n)} \right\|_2^2}. \quad (54)$$

711 Solution (54) can be evaluated without constructing  $\mathbf{R}_k^{<n>}$ . Observe that

$$712 \quad (\mathbf{b}_k^{(n)})^T \mathbf{b}_k^{(n)} = \prod_{\tilde{n}=1, \tilde{n} \neq n}^N (\mathbf{h}_k^{(\tilde{n})})^T \mathbf{h}_k^{(\tilde{n})}, \quad (55)$$

713

714 which is a simple case of (50), and

$$715 \quad \mathbf{R}_k^{<n>} \mathbf{b}_k^{(n)} = \left( \mathcal{A} - \sum_{\tilde{k}=1, \tilde{k} \neq k}^K \mathbf{h}_{\tilde{k}}^{(1)} \circ \dots \circ \mathbf{h}_{\tilde{k}}^{(N)} \right)^{<n>} \mathbf{b}_k^{(n)} \quad (56)$$

$$716 \quad = \mathbf{A}^{<n>} \mathbf{b}_k^{(n)} - \sum_{\tilde{k}=1, \tilde{k} \neq k}^K \left( \prod_{\tilde{n}=1, \tilde{n} \neq n}^N \left( \mathbf{h}_{\tilde{k}}^{(\tilde{n})} \right)^T \mathbf{h}_{\tilde{k}}^{(\tilde{n})} \right) \mathbf{h}_{\tilde{k}}^{(n)}. \quad (57)$$

720 Solution (54) can then be simplified as

$$721 \quad \mathbf{h}_k^{(n)} \leftarrow$$

$$722 \quad \left[ \mathbf{h}_k^{(n)} + \frac{\mathbf{A}^{<n>} \mathbf{b}_k^{(n)} - \mathbf{H}^{(n)} \left( \bigotimes_{\tilde{n}=1, \tilde{n} \neq n}^N \left( \mathbf{H}^{(\tilde{n})} \right)^T \mathbf{H}^{(\tilde{n})} \right) \cdot_k}{\prod_{\tilde{n}=1, \tilde{n} \neq n}^N \left( \mathbf{h}_k^{(\tilde{n})} \right)^T \mathbf{h}_k^{(\tilde{n})}} \right], \quad (58)$$

725 where  $\mathbf{A}^{<n>} \mathbf{b}_k^{(n)}$  can be computed using (49). Observe the similarity between (58) and (14).

726 **6 Implementation issues and comparisons**

727 **6.1 Stopping criterion**

728 Iterative methods have to be equipped with a criterion for stopping iterations. In NMF or  
 729 NTF, an ideal criterion would be to stop iterations after a local minimum of (2) or (45) is  
 730 attained. In practice, a few alternatives have been used.

731 Let us first discuss stopping criteria for NMF. A naive approach is to stop when the decrease  
 732 of the objective function becomes smaller than some predefined threshold:

$$733 \quad f(\mathbf{W}^{(i-1)}, \mathbf{H}^{(i-1)}) - f(\mathbf{W}^{(i)}, \mathbf{H}^{(i)}) \leq \epsilon, \quad (59)$$

735 where  $\epsilon$  is a tolerance value to choose. Although this method is commonly adopted, it is  
 736 potentially misleading because the decrease of the objective function may become small  
 737 before a local minimum is achieved. A more principled criterion was proposed by Lin as fol-  
 738 lows [71]. According to the Karush–Kuhn–Tucher (KKT) conditions,  $(\mathbf{W}, \mathbf{H})$  is a stationary  
 739 point of (2) if and only if [17]

$$740 \quad \mathbf{W} \geq 0, \quad \mathbf{H} \geq 0, \quad (60a)$$

$$742 \quad \nabla f_{\mathbf{W}} = \frac{\partial f(\mathbf{W}, \mathbf{H})}{\partial \mathbf{W}} \geq 0, \quad \nabla f_{\mathbf{H}} = \frac{\partial f(\mathbf{W}, \mathbf{H})}{\partial \mathbf{H}} \geq 0, \quad (60b)$$

$$746 \quad \mathbf{W} \otimes \nabla f_{\mathbf{W}} = 0, \quad \mathbf{H} \otimes \nabla f_{\mathbf{H}} = 0, \quad (60c)$$

748 where

$$749 \quad \nabla f_{\mathbf{W}} = 2\mathbf{W}\mathbf{H}^T\mathbf{H} - 2\mathbf{A}\mathbf{H} \text{ and}$$

$$750 \quad \nabla f_{\mathbf{H}} = 2\mathbf{H}\mathbf{W}^T\mathbf{W} - 2\mathbf{A}^T\mathbf{W}.$$

751 Define the projected gradient  $\nabla^p f_{\mathbf{W}} \in \mathbb{R}^{M \times K}$  as,

752 
$$(\nabla^p f_{\mathbf{W}})_{mk} \equiv \begin{cases} (\nabla f_{\mathbf{W}})_{mk} & \text{if } (\nabla f_{\mathbf{W}})_{mk} < 0 \text{ or } \mathbf{W}_{mk} > 0, \\ 0 & \text{otherwise,} \end{cases}$$

753 for  $m = 1, \dots, M$  and  $k = 1, \dots, K$ , and  $\nabla^p f_{\mathbf{H}}$  similarly. Then, conditions (60) can be  
754 rephrased as

755 
$$\nabla^p f_{\mathbf{W}} = \mathbf{0} \text{ and } \nabla^p f_{\mathbf{H}} = \mathbf{0}.$$

756 Denote the projected gradient matrices at the  $i$ th iteration by  $\nabla^p f_{\mathbf{W}}^{(i)}$  and  $\nabla^p f_{\mathbf{H}}^{(i)}$ , and define

757 
$$\Delta(i) = \sqrt{\|\nabla^p f_{\mathbf{W}}^{(i)}\|_F^2 + \|\nabla^p f_{\mathbf{H}}^{(i)}\|_F^2}. \tag{61}$$
  
758

759 Using this definition, the stopping criterion is written by

760 
$$\frac{\Delta(i)}{\Delta(0)} \leq \epsilon, \tag{62}$$
  
761

762 where  $\Delta(0)$  is from the initial values of  $(\mathbf{W}, \mathbf{H})$ . Unlike (59), (62) guarantees the stationarity  
763 of the final solution. Variants of this criterion was used in [40,53].

764 An analogous stopping criterion can be derived for the NCP formulation in (45).  
765 The gradient matrix  $\nabla f_{\mathbf{H}^{(n)}}$  can be derived from the least squares representation in (48):

766 
$$\nabla f_{\mathbf{H}^{(n)}} = 2\mathbf{H}^{(n)} (\mathbf{B}^{(n)})^T \mathbf{B}^{(n)} - 2\mathbf{A}^{<n>} \mathbf{B}^{(n)}.$$

767 See (49) and (50) for efficient computation of  $(\mathbf{B}^{(n)})^T \mathbf{B}^{(n)}$  and  $\mathbf{A}^{<n>} \mathbf{B}^{(n)}$ . With function  $\Delta$   
768 defined as

769 
$$\Delta(i) = \sqrt{\sum_{n=1}^N \|\nabla^p f_{\mathbf{H}^{(n)}}^{(i)}\|_F^2}, \tag{63}$$
  
770

771 criterion in (62) can be used to stop iterations of an NCP algorithm.

772 Using (59) or (62) for the purpose of comparing algorithms might be unreliable. One might  
773 want to measure the amounts of time until several algorithms satisfy one of these criteria and  
774 compare them [53,71]. Such comparison would usually reveal meaningful trends, but there  
775 are some caveats. The difficulty of using (59) is straightforward because, in some algorithm  
776 such as the multiplicative updating rule, the difference in (59) can become quite small before  
777 arriving at a minimum. The difficulty of using (62) is as follows. Note that the diagonal  
778 rescaling of  $\mathbf{W}$  and  $\mathbf{H}$  does not affect the quality of approximation: For a diagonal matrix  
779  $\mathbf{D} \in \mathbb{R}_+^{K \times K}$  with positive diagonal elements,  $\mathbf{WH}^T = \mathbf{WD}^{-1}(\mathbf{HD})^T$ . However, the norm of  
780 the projected gradients in (61) is affected by a diagonal scaling:

781 
$$\left( \frac{\partial f}{\partial(\mathbf{WD}^{-1})}, \frac{\partial f}{\partial(\mathbf{HD})} \right) = \left( \left( \frac{\partial f}{\partial \mathbf{W}} \right) \mathbf{D}, \left( \frac{\partial f}{\partial \mathbf{H}} \right) \mathbf{D}^{-1} \right).$$

782 Hence, two solutions that are only different up to a diagonal scaling have the same objective  
783 function value, but they can be measured differently in terms of the norm of the projected  
784 gradients. See Kim and Park [59] for more information. Ho [44] considered including a  
785 normalization step before computing (61) to avoid this issue.

## 786 6.2 Results of experimental comparisons

787 A number of papers have reported the results of experimental comparisons of NMF algo-  
 788 rithms. A few papers have shown the slow convergence of Lee and Seung's multiplicative  
 789 updating rule and demonstrated the superiority of other algorithms published subsequently  
 790 [40, 53, 71]. Comprehensive comparisons of several efficient algorithms for NMF were con-  
 791 ducted in Kim and Park [59], where MATLAB implementations of the ANLS-based methods,  
 792 the HALS/RRI method, the multiplicative updating rule, and a few others were compared.  
 793 In their results, the slow convergence of the multiplicative updating was confirmed, and the  
 794 ALS method in Sect. 3.3 was shown to fail to converge in many cases. Among all the meth-  
 795 ods tested, the HALS/RRI method and the ANLS/BPP method showed the fastest overall  
 796 convergence.

797 Further comparisons are presented in Gillis and Glineur [37] and Hsieh and Dhillon [48]  
 798 where the authors proposed acceleration methods for the HALS/RRI method. Their compar-  
 799 isons show that the HALS/RRI method or the accelerated versions converge the fastest among  
 800 all methods tested. Korattikara et al. [62] demonstrated an effective approach to accelerate  
 801 the ANLS/BPP method. Overall, the HALS/RRI method, the ANLS/BPP method, and their  
 802 accelerated versions show the state-of-the-art performance in the experimental comparisons.

803 Comparison results of algorithms for NCP are provided in [60]. Interestingly, the  
 804 ANLS/BPP method showed faster convergence than the HALS/RRI method in the ten-  
 805 sor factorization case. Further investigations and experimental evaluations of the NCP  
 806 algorithms are needed to fully explain these observations.

807 **7 Efficient NMF updating: algorithms**

808 In practice, we often need to update a factorization with a slightly modified condition or  
 809 some additional data. We consider two scenarios where an existing factorization needs to  
 810 be efficiently updated to a new factorization. Importantly, the unified view of the NMF  
 811 algorithms presented in earlier chapters provides useful insights when we choose algorithmic  
 812 components for updating. Although we focus on the NMF updating here, similar updating  
 813 schemes can be developed for NCP as well.

814 **7.1 Updating NMF with an increased or decreased  $K$** 

815 NMF algorithms discussed in Sects. 2 and 3 assume that  $K$ , the reduced dimension, is  
 816 provided as an input. In practical applications, however, prior knowledge on  $K$  might not be  
 817 available, and a proper value for  $K$  has to be determined from data. To determine  $K$  from  
 818 data, typically NMFs are computed for several different  $K$  values and then the best  $K$  is  
 819 chosen according to some criterion [10, 33, 49]. In this case, computing several NMFs each  
 820 time from scratch would be very expensive, and therefore it is desired to develop an algorithm  
 821 to efficiently update an already computed factorization. We propose an algorithm for this task  
 822 in this subsection.

823 Suppose we have computed  $\mathbf{W}_{old} \in \mathbb{R}_+^{M \times K_1}$  and  $\mathbf{H}_{old} \in \mathbb{R}_+^{N \times K_1}$  as a solution of (2) with  
 824  $K = K_1$ . For  $K = K_2$  which is close to  $K_1$ , we are to compute new factors  $\mathbf{W}_{new} \in \mathbb{R}_+^{M \times K_2}$   
 825 and  $\mathbf{H}_{new} \in \mathbb{R}_+^{N \times K_2}$  as a minimizer of (2). Let us first consider the  $K_2 > K_1$  case, which is  
 826 shown in Fig. 2. Each of  $\mathbf{W}_{new}$  and  $\mathbf{H}_{new}$  in this case contains  $K_2 - K_1$  additional columns  
 827 compared to  $\mathbf{W}_{old}$  and  $\mathbf{H}_{old}$ . A natural strategy is to initialize new factor matrices by recycling  
 828  $\mathbf{W}_{old}$  and  $\mathbf{H}_{old}$  as

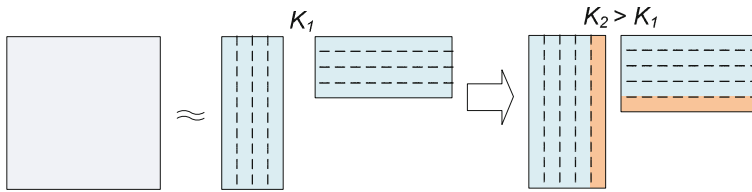


Fig. 2 Updating NMF with an increased  $K$

$$\mathbf{W}_{new} = [\mathbf{W}_{old} \ \mathbf{W}_{add}] \text{ and } \mathbf{H}_{new} = [\mathbf{H}_{old} \ \mathbf{H}_{add}], \tag{64}$$

where  $\mathbf{W}_{add} \in \mathbb{R}_+^{M \times (K_2 - K_1)}$  and  $\mathbf{H}_{add} \in \mathbb{R}_+^{N \times (K_2 - K_1)}$  are generated with, e.g., random non-negative entries. Using (64) as initial values, we can execute an NMF algorithm to find the solution of (2). Since  $\mathbf{W}_{old}$  and  $\mathbf{H}_{old}$  already approximate  $\mathbf{A}$ , this warm-start strategy is expected to be more efficient than computing everything from scratch.

We further improve this strategy based on the following observation. Instead of initializing  $\mathbf{W}_{add}$  and  $\mathbf{H}_{add}$  with random entries, we can compute  $\mathbf{W}_{add}$  and  $\mathbf{H}_{add}$  that approximately factorize the residual matrix, i.e.,  $\mathbf{A} - \mathbf{W}_{old} \mathbf{H}_{old}^T$ . This can be done by solving the following problem:

$$\begin{aligned} & (\mathbf{W}_{add}, \mathbf{H}_{add}) \leftarrow \\ & \arg \min_{\substack{\mathbf{W} \in \mathbb{R}^{M \times (K_2 - K_1)} \\ \mathbf{H} \in \mathbb{R}^{N \times (K_2 - K_1)}}} \left\| (\mathbf{A} - \mathbf{W}_{old} \mathbf{H}_{old}^T) - \mathbf{W} \mathbf{H}^T \right\|_F^2 \\ & \text{subject to } \mathbf{W} \geq 0, \mathbf{H} \geq 0. \end{aligned} \tag{65}$$

Problem (65) need not be solved very accurately. Once an approximate solution is obtained, it is used to initialize  $\mathbf{W}_{new}$  and  $\mathbf{H}_{new}$  in (64) and then an NMF algorithm is executed for entire matrices  $\mathbf{W}_{new}$  and  $\mathbf{H}_{new}$ .

When  $K_2 < K_1$ , we need less columns in  $\mathbf{W}_{new}$  and  $\mathbf{H}_{new}$  than in  $\mathbf{W}_{old}$  and  $\mathbf{H}_{old}$ . For a good initialization of  $\mathbf{W}_{new}$  and  $\mathbf{H}_{new}$ , we need to choose the columns from  $\mathbf{W}_{old}$  and  $\mathbf{H}_{old}$ . Observing that

$$\mathbf{A} \approx \mathbf{W}_{old} \mathbf{H}_{old}^T = \sum_{k=1}^{K_1} (\mathbf{W}_{old})_{\cdot k} (\mathbf{H}_{old})_{\cdot k}^T, \tag{66}$$

$K_2$  columns can be selected as follows. Let  $\delta_k$  be the squared Frobenius norm of the  $k$ th rank-one matrix in (66), given as

$$\delta_k = \| (\mathbf{W}_{old})_{\cdot k} (\mathbf{H}_{old})_{\cdot k}^T \|_F^2 = \| (\mathbf{W}_{old})_{\cdot k} \|_2^2 \| (\mathbf{H}_{old})_{\cdot k} \|_2^2.$$

We then take the largest  $K_2$  values from  $\delta_1, \dots, \delta_{K_1}$  and use corresponding columns of  $\mathbf{W}_{old}$  and  $\mathbf{H}_{old}$  as initializations for  $\mathbf{W}_{new}$  and  $\mathbf{H}_{new}$ .

Summarizing the two cases, an algorithm for updating NMF with an increased or decreased  $K$  value is presented in Algorithm 2. Note that the HALS/RR1 method is chosen for Step 2: Since the new entries appear as column blocks (see Fig. 2), the HALS/RR1 method is an optimal choice. For Step 2, although any algorithm may be chosen, we have adopted the HALS/RR1 method for our experimental evaluation in Sect. 8.1.

**Algorithm 2** Updating NMF with Increased or Decreased  $K$  Values

**Input:**  $\mathbf{A} \in \mathbb{R}_+^{M \times N}$ ,  $(\mathbf{W}_{old} \in \mathbb{R}_+^{M \times K_1}, \mathbf{H}_{old} \in \mathbb{R}_+^{N \times K_1})$  as a minimizer of (2), and  $K_2$ .

**Output:**  $(\mathbf{W}_{new} \in \mathbb{R}_+^{M \times K_2}, \mathbf{H}_{new} \in \mathbb{R}_+^{N \times K_2})$  as a minimizer of (2).

- 1: **if**  $K_2 > K_1$  **then**
- 2:   Approximately solve (65) with the HALS/RRI method to find  $(\mathbf{W}_{add}, \mathbf{H}_{add})$ .
- 3:   Let  $\mathbf{W}_{new} \leftarrow [\mathbf{W}_{old} \ \mathbf{W}_{add}]$  and  $\mathbf{H}_{new} \leftarrow [\mathbf{H}_{old} \ \mathbf{H}_{add}]$ .
- 4: **end if**
- 5: **if**  $K_2 < K_1$  **then**
- 6:   For  $k = 1, \dots, K_1$ , let

$$\delta_k = \|(\mathbf{W}_{old})_{\cdot k}\|_2^2 \|(\mathbf{H}_{old})_{\cdot k}\|_2^2.$$

- 7:   Let  $J$  be the indices corresponding to the  $K_2$  largest values of  $\delta_1, \dots, \delta_{K_1}$ .
- 8:   Let  $\mathbf{W}_{new}$  and  $\mathbf{H}_{new}$  be the submatrices of  $\mathbf{W}_{old}$  and  $\mathbf{H}_{old}$  obtained from the columns indexed by  $J$ .
- 9: **end if**
- 10: Using  $\mathbf{W}_{new}$  and  $\mathbf{H}_{new}$  as initial values, execute an NMF algorithm to compute NMF of  $\mathbf{A}$ .

863 7.2 Updating NMF with incremental data

864 In applications such as video analysis and mining of text stream, we have to deal with dynamic  
 865 data where new data keep coming in and obsolete data get discarded. Instead of completely  
 866 recomputing the factorization after only a small portion of data are updated, an efficient  
 867 algorithm needs to be designed to update NMF. Let us first consider a case that new data are  
 868 observed, as shown in Fig. 3. Suppose we have computed  $\mathbf{W}_{old} \in \mathbb{R}_+^{M \times K}$  and  $\mathbf{H}_{old} \in \mathbb{R}_+^{N \times K}$   
 869 as a minimizer of (2) for  $\mathbf{A} \in \mathbb{R}_+^{M \times N}$ . New data,  $\Delta \mathbf{A} \in \mathbb{R}_+^{M \times \Delta N}$ , are placed in the last  
 870 columns of a new matrix as  $\tilde{\mathbf{A}} = [\mathbf{A} \ \Delta \mathbf{A}]$ . Our goal is to efficiently compute the updated  
 871 NMF

$$\tilde{\mathbf{A}} = [\mathbf{A} \ \Delta \mathbf{A}] \approx \mathbf{W}_{new} \mathbf{H}_{new}^T,$$

872 where  $\mathbf{W}_{new} \in \mathbb{R}_+^{M \times K}$  and  $\mathbf{H}_{new} \in \mathbb{R}_+^{(N+\Delta N) \times K}$ .

873 The following strategy we propose is simple but efficient. Since columns in  $\mathbf{W}_{old}$  form  
 874 a basis whose nonnegative combinations approximate  $\mathbf{A}$ , it is reasonable to use  $\mathbf{W}_{old}$  to  
 875 initialize  $\mathbf{W}_{new}$ . Similarly,  $\mathbf{H}_{new}$  is initialized as  $\begin{bmatrix} \mathbf{H}_{old} \\ \Delta \mathbf{H} \end{bmatrix}$  where the first part,  $\mathbf{H}_{old}$ , is obtained  
 876 from the existing factorization. A new coefficient submatrix,  $\Delta \mathbf{H} \in \mathbb{R}_+^{\Delta N \times K}$ , is needed to  
 877 represent the coefficients for new data. Although it is possible to initialize  $\Delta \mathbf{H}$  with random  
 878 entries, an improved approach is to solve the following NLS problem:  
 879

$$\Delta \mathbf{H} \leftarrow \arg \min_{\mathbf{H} \in \mathbb{R}^{\Delta N \times K}} \|\mathbf{W}_{old} \mathbf{H}^T - \Delta \mathbf{A}\|_F^2 \text{ s.t. } \mathbf{H} \geq 0. \tag{67}$$

880  
 881  
 882 Using these initializations, we can then execute an NMF algorithm to find an optimal solution  
 883 for  $\mathbf{W}_{new}$  and  $\mathbf{H}_{new}$ . Various algorithms for the NLS problem, discussed in Sect. 4, maybe  
 884 used to solve (67). In order to achieve optimal efficiency, due to the fact that the number  
 885 of rows of  $\Delta \mathbf{H}^T$  is usually small, the block principal pivoting algorithm is one of the most  
 886 efficient method as demonstrated in [59]. We summarize this method for updating NMF with  
 887 incremental data in Algorithm 3.

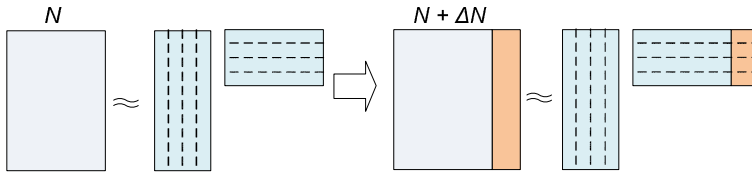


Fig. 3 Updating NMF with incremental data

**Algorithm 3** Updating NMF with Incremental Data

**Input:**  $\mathbf{A} \in \mathbb{R}_+^{M \times N}$ ,  $(\mathbf{W}_{old} \in \mathbb{R}_+^{M \times K}, \mathbf{H}_{old} \in \mathbb{R}_+^{N \times K})$  as a solution of Eq. (2), and  $\Delta \mathbf{A} \in \mathbb{R}_+^{M \times \Delta N}$ .

**Output:**  $\mathbf{W}_{new} \in \mathbb{R}_+^{M \times K}$  and  $\mathbf{H}_{new} \in \mathbb{R}_+^{(N+\Delta N) \times K}$  as a solution of Eq. (2).

1: Solve the following NLS problem:

$$\Delta \mathbf{H} \leftarrow \arg \min_{\mathbf{H} \in \mathbb{R}^{\Delta N \times K}} \|\mathbf{W}_{old} \mathbf{H}^T - \Delta \mathbf{A}\|_F^2 \text{ s.t. } \mathbf{H} \geq 0.$$

2: Let  $\mathbf{W}_{new} \leftarrow \mathbf{W}_{old}$  and  $\mathbf{H}_{new} \leftarrow \begin{bmatrix} \mathbf{H}_{old} \\ \Delta \mathbf{H} \end{bmatrix}$ .

3: Using  $\mathbf{W}_{new}$  and  $\mathbf{H}_{new}$  as initial values, execute an NMF algorithm to compute NMF of  $[\mathbf{A} \ \Delta \mathbf{A}]$ .

888 Deleting obsolete data is easier. If  $\mathbf{A} = [\Delta \mathbf{A} \tilde{\mathbf{A}}]$  where  $\Delta \mathbf{A} \in \mathbb{R}_+^{M \times \Delta N}$  is to be discarded,  
 889 we similarly divide  $\mathbf{H}_{old}$  as  $\mathbf{H}_{old} = \begin{bmatrix} \Delta \mathbf{H} \\ \tilde{\mathbf{H}}_{old} \end{bmatrix}$ . We then use  $\mathbf{W}_{old}$  and  $\tilde{\mathbf{H}}_{old}$  to initialize  $\mathbf{W}_{new}$   
 890 and  $\mathbf{H}_{new}$  and execute an NMF algorithm to find a minimizer of (2).

891 **8 Efficient NMF updating: experiments and applications**

892 We provide the experimental validations of the effectiveness of Algorithms 2 and 3 and show  
 893 their applications. The computational efficiency was compared on dense and sparse synthetic  
 894 matrices as well as on real-world data sets. All the experiments were executed with MATLAB  
 895 on a Linux machine with 2GHz Intel Quad-core processor and 4GB memory.

896 **8.1 Comparisons of NMF updating methods for varying K**

897 We compared Algorithm 2 with two alternative methods for updating NMF. The first method  
 898 is to compute NMF with  $K = K_2$  from scratch using the HALS/RRI algorithm, which  
 899 we denote as ‘recompute’ in our figures. The second method, denoted as ‘warm-restart’  
 900 in the figures, computes the new factorization as follows. If  $K_2 > K_1$ , it generates  $\mathbf{W}_{add} \in$   
 901  $\mathbb{R}_+^{M \times (K_2 - K_1)}$  and  $\mathbf{H}_{add} \in \mathbb{R}_+^{N \times (K_2 - K_1)}$  using random entries to initialize  $\mathbf{W}_{new}$  and  $\mathbf{H}_{new}$   
 902 as in (64). If  $K_2 < K_1$ , it randomly selects  $K_2$  pairs of columns from  $\mathbf{W}_{old}$  and  $\mathbf{H}_{old}$   
 903 to initialize the new factors. Using these initializations, ‘warm-restart’ executes the HALS/RRI  
 904 algorithm to finish the NMF computation.

905 Synthetic data sets and performance comparisons on them are as follows. We created both  
 906 dense and sparse matrices. For dense matrices, we generated  $\mathbf{W} \in \mathbb{R}_+^{M \times K}$  and  $\mathbf{H} \in \mathbb{R}_+^{N \times K}$   
 907 with random entries and computed  $\mathbf{A} = \mathbf{W}\mathbf{H}^T$ . Then, Gaussian noise was added to the  
 908 elements of  $\mathbf{A}$  where the noise has zero mean and standard deviation is 5% of the average  
 909 magnitude of elements in  $\mathbf{A}$ . All negative elements after adding the noise were set to zero.

We generated a  $600 \times 600$  dense matrix with  $K = 80$ . For sparse matrices, we first generated  $\mathbf{W} \in \mathbb{R}_+^{M \times K}$  and  $\mathbf{H} \in \mathbb{R}_+^{N \times K}$  with 90% sparsity and computed  $\mathbf{A} = \mathbf{WH}^T$ . We then used a soft-thresholding operation to obtain a sparse matrix  $\mathbf{A}$ ,<sup>1</sup> and the resulting matrix had 88.2% sparsity. We generated a synthetic sparse matrix of size  $3,000 \times 3,000$ .<sup>2</sup> In order to observe efficiency in updating, an NMF with  $K_1 = 60$  was first computed and stored. We then computed NMFs with  $K_2 = 50, 65$ , and  $80$ . The plots of relative error vs. execution time for all three methods are shown in Fig. 4. Our proposed method achieved faster convergence compared to ‘warm-restart’ and ‘recompute’, which sometimes required several times more computation to achieve the same accuracy as our method. The advantage of the proposed method can be seen in both dense and sparse cases.

We have also used four real-world data sets for our comparisons. From the Topic Detection and Tracking 2 (TDT2) text corpus,<sup>3</sup> we selected 40 topics to create a sparse term-document matrix of size  $19,009 \times 3,087$ . From the 20 Newsgroups data set,<sup>4</sup> a sparse term-document matrix of size  $7,845 \times 11,269$  was obtained after removing keywords and documents with frequency less than 20. The AT&T facial image database<sup>5</sup> produced a dense matrix of size  $10,304 \times 400$ . The images in the CMU PIE database<sup>6</sup> were resized to  $64 \times 64$  pixels, and we formed a dense matrix of size  $4,096 \times 11,554$ .<sup>7</sup> We focused on the case when  $K$  increases, and the results are reported in Fig. 5. As with the synthetic data sets, our proposed method was shown to be the most efficient among the methods we tested.

## 8.2 Applications of NMF updating for varying $K$

Algorithm 2 can be used to determine the reduced dimension,  $K$ , from data. Our first example, shown in Fig. 6a, is determining a proper  $K$  value that represents the number of clusters. Using NMF as a clustering method [57, 63], Brunet et al. [10] proposed to select the number of clusters by computing NMFs with multiple initializations for various  $K$  values and then evaluating the dispersion coefficients (See [10, 52, 57] for more details). We took the MNIST digit image database [65] and used 500 images with  $28 \times 28$  pixels from each of the digits 6, 7, 8, and 9. The resulting data matrix was of size  $784 \times 2,000$ . We computed NMFs for  $K = 3, 4, 5$ , and  $6$  with 50 different initializations for each  $K$ . The top of Fig. 6a shows that  $K = 4$  can be correctly determined from the point where the dispersion coefficient starts to drop. The bottom of Fig. 6a shows the box-plot of the total execution time needed by Algorithm 2, ‘recompute’, and ‘warm-restart’. We applied the same stopping criterion in (62) for all three methods.

Further applications of Algorithm 2 are shown in Fig. 6b, c. Figure 6b demonstrates a process of probing the approximation errors of NMF with various  $K$  values. With  $K = 20, 40, 60$  and  $80$ , we generated  $600 \times 600$  synthetic dense matrices as described in Sect. 8.1. Then, we computed NMFs with Algorithm 2 for  $K$  values ranging from 10 to 160 with a step size 5. The relative objective function values with respect to  $K$  are shown in Fig. 6b. In each of the cases where  $K = 20, 40, 60$ , and  $80$ , we were able to determine the correct  $K$  value by choosing a point where the relative error stopped decreasing significantly.

<sup>1</sup> For each element  $a_{ij}$ , we used  $a_{ij} \leftarrow \max(a_{ij} - 2, 0)$ .

<sup>2</sup> We created a larger matrix for the sparse case to clearly illustrate the relative efficiency.

<sup>3</sup> <http://projects.ldc.upenn.edu/TDT2/>.

<sup>4</sup> <http://people.csail.mit.edu/jrennie/20Newsgroups/>.

<sup>5</sup> <http://www.cl.cam.ac.uk/research/dtg/attarchive/facedatabase.html>.

<sup>6</sup> [http://www.ri.cmu.edu/projects/project\\_418.html](http://www.ri.cmu.edu/projects/project_418.html).

<sup>7</sup> <http://www.zjucadcg.cn/dengcai/Data/FaceData.html>.

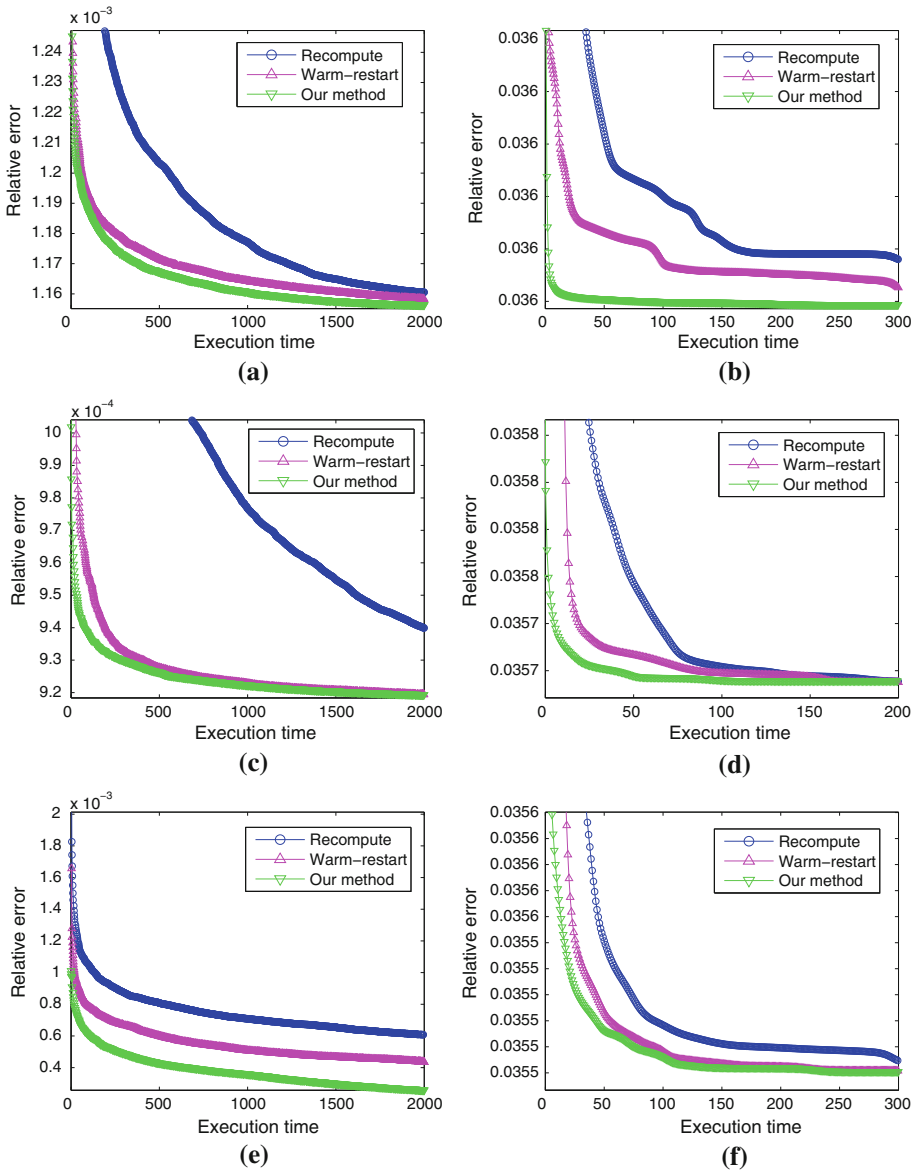


**Fig. 4** Comparisons of updating and recomputing methods for NMF when  $K$  changes, using synthetic matrices. The relative error represents  $\|A - WH^T\|_F / \|A\|_F$ , and time was measured in seconds. The dense matrix was of size  $600 \times 600$ , and the sparse matrix was of size  $3,000 \times 3,000$ . See text for more details. **a** Dense,  $K : 60 \rightarrow 60$ . **b** Sparse,  $K : 60 \rightarrow 50$ . **c** Dense,  $K : 60 \rightarrow 65$ . **d** Sparse,  $K : 60 \rightarrow 65$ . **e** Dense,  $K : 60 \rightarrow 80$ . **f** Sparse,  $K : 60 \rightarrow 80$

949 Figure 6c demonstrates the process of choosing  $K$  for a classification purpose. Using the  
 950  $10,304 \times 400$  matrix from the AT&T facial image database, we computed NMF to generate  
 951 a  $K$  dimensional representation of each image, taken from each row of  $H$ . We then trained a  
 952 nearest neighbor classifier using the reduced-dimensional representations [83]. To determine

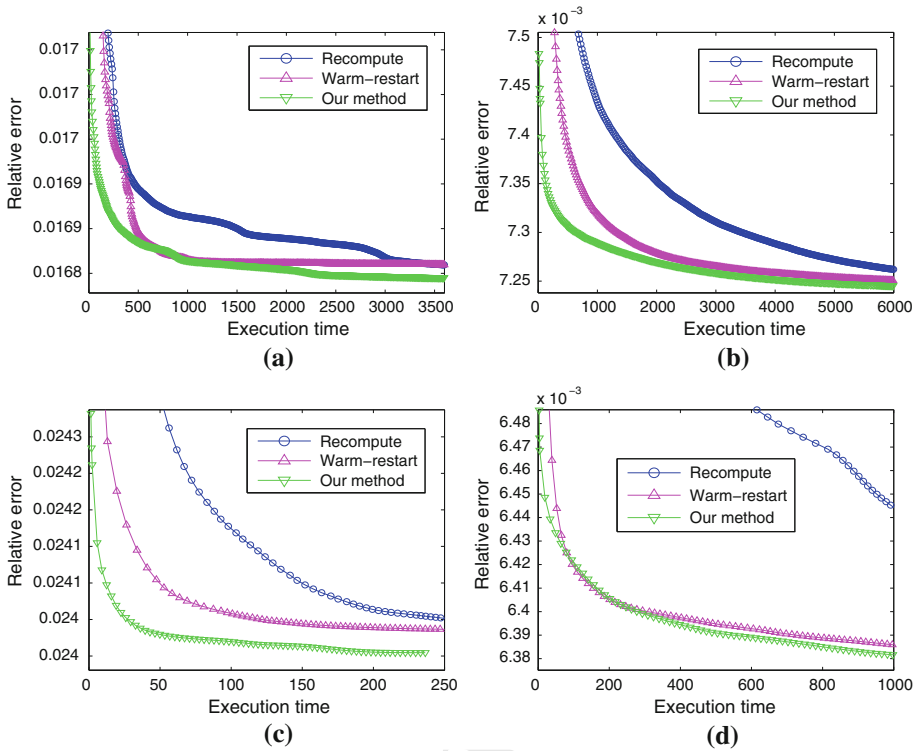


**Fig. 5** Comparisons of updating and recomputing methods for NMF when  $K$  changes, using real-world data sets. The relative error represents  $\|\mathbf{A} - \mathbf{W}\mathbf{H}^T\|_F / \|\mathbf{A}\|_F$ , and time was measured in seconds. The AT&T and the PIE data sets were dense matrices of size  $10,304 \times 400$  and  $4,096 \times 11,554$ , respectively. The TDT2 and the 20 Newsgroup data sets were sparse matrices of size  $19,009 \times 3,087$  and  $7,845 \times 11,269$ , respectively. **a** AT&T, dense,  $K : 80 \rightarrow 100$ , **b** PIE, dense,  $K : 80 \rightarrow 100$ , **c** TDT2, sparse,  $K : 160 \rightarrow 200$ , **d** 20 Newsgroup, sparse,  $K : 160 \rightarrow 200$

953 the best  $K$  value, we performed the 5-fold cross validation: Each time a data matrix of size  
 954  $10,304 \times 320$  was used to compute  $\mathbf{W}$  and  $\mathbf{H}$ , and the reduced-dimensional representations for  
 955 the test data  $\tilde{\mathbf{A}}$  were obtained by solving a NLS problem,  $\min_{\mathbf{H} \geq 0} \|\tilde{\mathbf{A}} - \mathbf{W}\mathbf{H}\|_F^2$ . Classification  
 956 errors on both training and testing sets are shown in Fig. 6c. Five paths of training and testing  
 957 errors are plotted using thin lines, and the averaged training and testing errors are plotted using  
 958 thick lines. Based on the figure, we chose  $K = 13$  since the testing error barely decreased  
 959 beyond the point whereas the training error approached zero.

960 **8.3 Comparisons of NMF updating methods for incremental data**

961 We also tested the effectiveness of Algorithm 3. We created a  $1,000 \times 500$  dense matrix  
 962  $\mathbf{A}$  as described in Sect. 8.1 with  $K = 100$ . An initial NMF with  $K = 80$  was computed  
 963 and stored. Then, an additional data set of size  $1,000 \times 10, 1,000 \times 20$ , or  $1,000 \times 50$  was  
 964 appended, and we computed the updated NMF with several methods as follows. In addition  
 965 to Algorithm 3, we considered four alternative methods. A naive approach that computes  
 966 the entire NMF from scratch is denoted as ‘recompute’. An approach that initializes a new

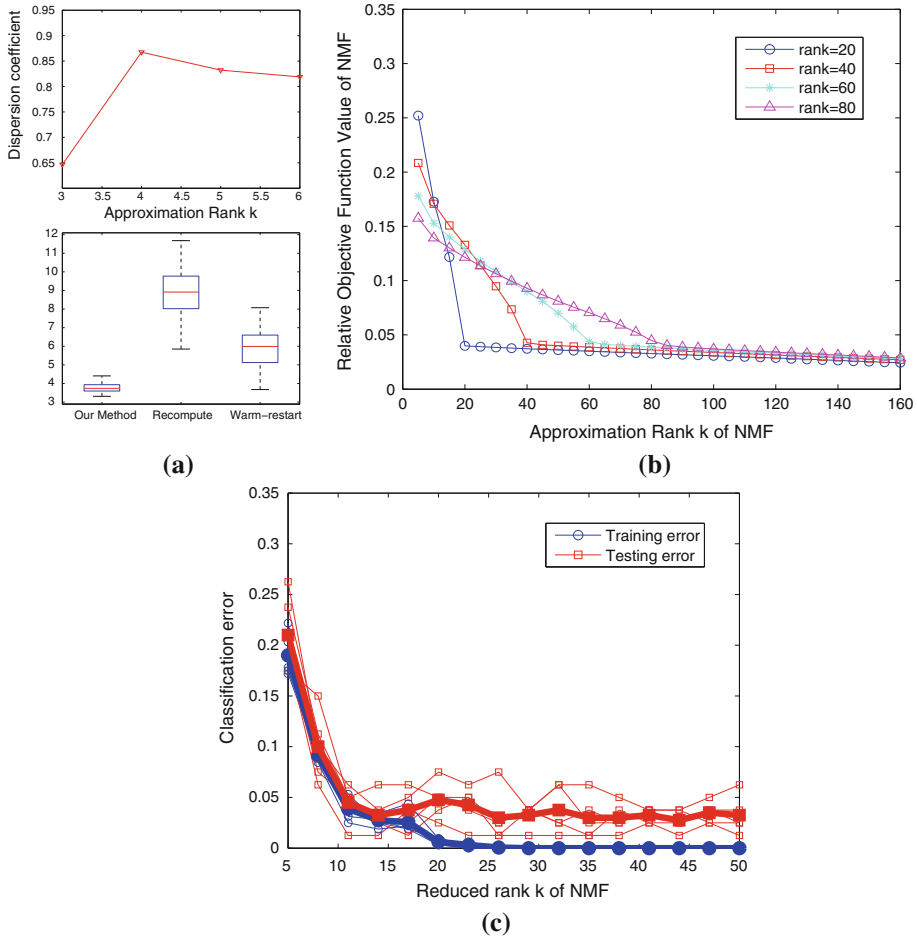


**Fig. 6** **a** Top Dispersion coefficients (see [10,57]) obtained by using 50 different initializations for each  $K$ , Bottom Execution time needed by our method, ‘recompute’, and ‘warm-restart’. **b** Relative errors for various  $K$  values on data sets created with  $K = 20, 40, 60$  and  $80$ . **c** Classification errors on training and testing data sets of AT&T facial image database using 5-fold cross validation

967 coefficient matrix as  $\mathbf{H}_{new} = \begin{bmatrix} \mathbf{H}_{old} \\ \Delta\mathbf{H} \end{bmatrix}$  where  $\Delta\mathbf{H}$  is generated with random entries is denoted  
 968 as ‘warm-restart’. The incremental NMF algorithm (INMF) [11] as well as the online NMF  
 969 algorithm (ONMF) [13] were also included in the comparisons. Figure 7 shows the execution  
 970 results, where our proposed method outperforms other methods tested.

971 **9 Conclusion and discussion**

972 We have reviewed algorithmic strategies for computing NMF and NTF from a unifying  
 973 perspective based on the BCD framework. The BCD framework for NMF and NTF enables  
 974 simplified understanding of several successful algorithms such as the alternating nonnegative  
 975 least squares (ANLS) and the hierarchical alternating least squares (HALS) methods. Based

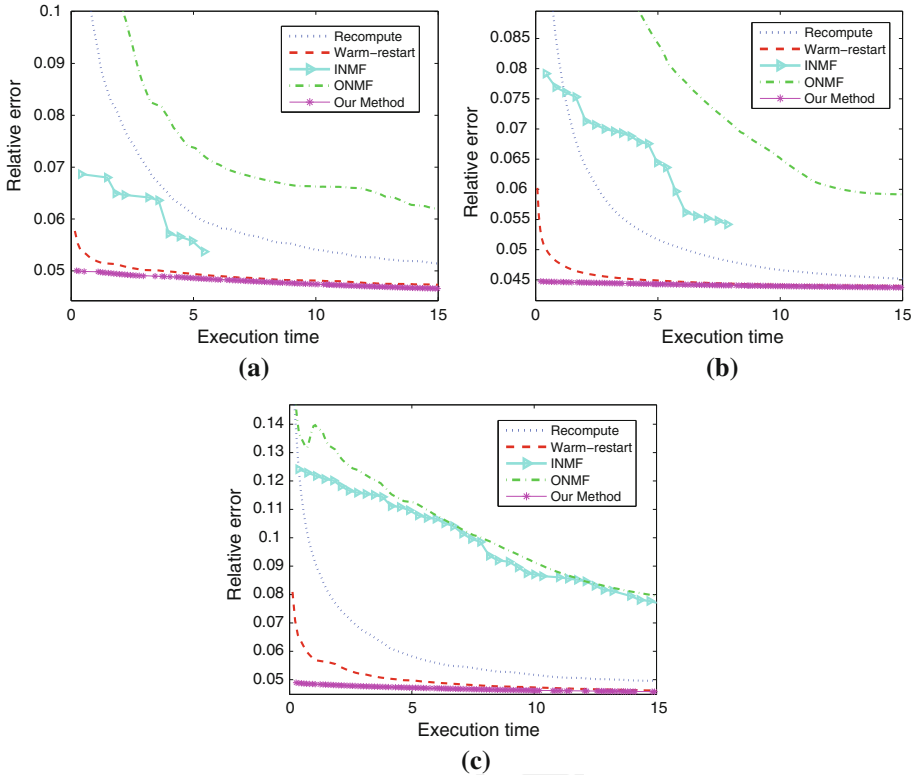


**Fig. 7** Comparisons of NMF updating methods for incremental data. Given a  $1,000 \times 500$  matrix and a corresponding NMF,  $\Delta N$  additional data items were appended and the NMF was updated. The relative error represents  $\|\mathbf{A} - \mathbf{W}\mathbf{H}^T\|_F / \|\mathbf{A}\|_F$ , and time was measured in seconds. **a**  $\Delta N = 10$ , **b**  $\Delta N = 20$ , **c**  $\Delta N = 50$

976 on the BCD framework, the theoretical convergence properties of the ANLS and the HALS  
 977 methods are readily explained. We have also summarized how previous algorithms that do  
 978 not fit in the BCD framework differ from the BCD-based methods. With insights from the  
 979 unified view, we proposed efficient algorithms for updating NMF both for the cases that the  
 980 reduced dimension varies and that data are incrementally added or discarded.

981 There are many other interesting aspects of NMF that are not covered in this paper. Depend-  
 982 ing on the probabilistic model of the underlying data, NMF can be formulated with various  
 983 divergences. Formulations and algorithms based on Kullback-Leibler divergence [67, 79],  
 984 Bregman divergence [24, 68], Itakura-Saito divergence [29], and Alpha and Beta divergences  
 985 [21, 22] have been developed. For discussion on nonnegative rank as well as the geometric  
 986 interpretation of NMF, see Lin and Chu [72], Gillis [34], and Donoho and Stodden [27].  
 987 NMF has been also studied from the Bayesian statistics point of view: See Schmidt et al.  
 988 [78] and Zhong and Girolami [88]. In the data mining community, variants of NMF such as  
 989 convex and semi-NMFs [25, 75], orthogonal tri-NMF [26], and group-sparse NMF [56] have  
 990 been proposed, and using NMF for clustering has been shown to be successful [12, 57, 63].  
 991 For an overview on the use of NMF in bioinformatics, see Devarajan [23] and references  
 992 therein. Cichocki et al.'s book [22] explains the use of NMF for signal processing. See Chu

993 and Plemmons [17], Berry et al. [4], and Cichocki et al. [22] for earlier surveys on NMF. See  
 994 also Ph.D. dissertations on NMF algorithms and applications [34,44,55].  
 995

996 **Open Access** This article is distributed under the terms of the Creative Commons Attribution License which  
 997 permits any use, distribution, and reproduction in any medium, provided the original author(s) and the source  
 998 are credited.

## 999 References

- 1000 1. Acar, E., Yener, B.: Unsupervised multiway data analysis: a literature survey. *IEEE Trans. Knowl. Data*  
 1001 *Eng.* **21**(1), 6–20 (2009)
- 1002 2. Bellavia, S., Macconi, M., Morini, B.: An interior point newton-like method for non-negative least-squares  
 1003 problems with degenerate solution. *Numer. Linear Algebra Appl.* **13**(10), 825–846 (2006)
- 1004 3. Berman, A., Plemmons, R.J.: *Nonnegative matrices in the mathematical sciences*. Society for Industrial  
 1005 and Applied Mathematics, Philadelphia (1994)
- 1006 4. Berry, M., Browne, M., Langville, A., Pauca, V., Plemmons, R.: Algorithms and applications for approx-  
 1007 imate nonnegative matrix factorization. *Comput. Stat. Data Anal.* **52**(1), 155–173 (2007)
- 1008 5. Bertsekas, D.P.: *Nonlinear programming*. Athena Scientific (1999)
- 1009 6. Biggs, M., Ghodsi, A., Vavasis, S.: Nonnegative matrix factorization via rank-one downdate. In: Proceed-  
 1010 ings of the 25th International Conference on, Machine Learning, pp. 64–71 (2008)
- 1011 7. Birgin, E., Martínez, J., Raydan, M.: Nonmonotone spectral projected gradient methods on convex sets.  
 1012 *SIAM J. Optim.* **10**(4), 1196–1211 (2000)
- 1013 8. Björck, Å.: *Numerical Methods for Least Squares Problems*. Society for Industrial and Applied Mathe-  
 1014 matics, Philadelphia (1996)
- 1015 9. Bro, R., De Jong, S.: A fast non-negativity-constrained least squares algorithm. *J. Chemom.* **11**, 393–401  
 1016 (1997)
- 1017 10. Brunet, J., Tamayo, P., Golub, T., Mesirov, J.: Metagenes and molecular pattern discovery using matrix  
 1018 factorization. *Proc. Natl. Acad. Sci.* **101**(12), 4164–4169 (2004)
- 1019 11. Bucak, S., Gunsul, B.: Video content representation by incremental non-negative matrix factoriza-  
 1020 tion. In: Proceedings of the 2007 IEEE International Conference on Image Processing (ICIP), vol. 2,  
 1021 pp. II-113–II-116 (2007)
- 1022 12. Cai, D., He, X., Han, J., Huang, T.: Graph regularized nonnegative matrix factorization for data represen-  
 1023 tation. *IEEE Trans. Pattern Anal. Mach. Intell.* **33**(8), 1548–1560 (2011)
- 1024 13. Cao, B., Shen, D., Sun, J.T., Wang, X., Yang, Q., Chen, Z.: Detect and track latent factors with online  
 1025 nonnegative matrix factorization. In: Proceedings of the 20th International Joint Conference on Artificial,  
 1026 Intelligence, pp. 2689–2694 (2007)
- 1027 14. Carroll, J.D., Chang, J.J.: Analysis of individual differences in multidimensional scaling via an n-way  
 1028 generalization of "eckart-young" decomposition. *Psychometrika* **35**(3), 283–319 (1970)
- 1029 15. Chen, D., Plemmons, R.J.: Nonnegativity constraints in numerical analysis. In: Proceedings of the  
 1030 Symposium on the Birth of Numerical Analysis, Leuven Belgium, pp. 109–140 (2009)
- 1031 16. Chen, S.S., Donoho, D.L., Saunders, M.A.: Atomic decomposition by basis pursuit. *SIAM Rev.* **43**(1),  
 1032 129–159 (2001)
- 1033 17. Chu, M., Plemmons, R.: Nonnegative matrix factorization and applications. *IMAGE: Bull. Int. Linear*  
 1034 *Algebra Soc.* **34**, 2–7 (2005)
- 1035 18. Chu, M.T., Lin, M.M.: Low-dimensional polytope approximation and its applications to nonnegative  
 1036 matrix factorization. *SIAM J. Sci. Comput.* **30**(3), 1131–1155 (2008)
- 1037 19. Cichocki, A., Phan, A.H.: Fast local algorithms for large scale nonnegative matrix and tensor factoriza-  
 1038 tions. *IEICE Trans. Fundam. Electron. Commun. Comput. Sci.* **E92-A**(3), 708–721 (2009)
- 1039 20. Cichocki, A., Zdunek, R., Amari, S.I.: Hierarchical ALS algorithms for nonnegative matrix and 3d tensor  
 1040 factorization. In: *Lecture Notes in Computer Science*, vol. 4666, pp. 169–176. Springer (2007)
- 1041 21. Cichocki, A., Zdunek, R., Choi, S., Plemmons, R., Amari, S.-I.: Nonnegative tensor factorization using  
 1042 alpha and beta divergencies. In: Proceedings of the 32nd International Conference on Acoustics, Speech,  
 1043 and Signal Processing (ICASSP), Honolulu, April 2007, vol. 3, pp. III-1393–III-1396 (2007)
- 1044 22. Cichocki, A., Zdunek, R., Phan, A.H., Amari, S.I.: *Nonnegative Matrix and Tensor Factorizations: Appli-  
 1045 cations to Exploratory Multi-Way Data Analysis and Blind Source Separation*. Wiley, West Sussex (2009)
- 1046 23. Devarajan, K.: Nonnegative matrix factorization: an analytical and interpretive tool in computational  
 1047 biology. *PLoS Comput. Biol.* **4**(7), e1000,029 (2008)

- 1048 24. Dhillon, I., Sra, S.: Generalized nonnegative matrix approximations with bregman divergences. In:  
1049 Advances in Neural Information Processing Systems 18, pp. 283–290. MIT Press (2006)
- 1050 25. Ding, C., Li, T., Jordan, M.: Convex and semi-nonnegative matrix factorizations. *IEEE Trans. Pattern*  
1051 *Anal. Mach. Intell.* **32**(1), 45–559 (2010)
- 1052 26. Ding, C., Li, T., Peng, W., Park, H.: Orthogonal nonnegative matrix tri-factorizations for clustering. In:  
1053 Proceedings of the 12th ACM SIGKDD International Conference on Knowledge Discovery and Data  
1054 Mining, pp. 126–135 (2006)
- 1055 27. Donoho, D., Stodden, V.: When does non-negative matrix factorization give a correct decomposition into  
1056 parts? In: Advances in Neural Information Processing Systems 16. MIT Press (2004)
- 1057 28. Drake, B., Kim, J., Mallick, M., Park, H.: Supervised Raman spectra estimation based on nonnegative  
1058 rank deficient least squares. In: Proceedings of the 13th International Conference on Information Fusion,  
1059 Edinburgh, UK (2010)
- 1060 29. Févotte, C., Bertin, N., Durrieu, J.: Nonnegative matrix factorization with the Itakura-Saito divergence:  
1061 With application to music analysis. *Neural Comput.* **21**(3), 793–830 (2009)
- 1062 30. Figueiredo, M.A.T., Nowak, R.D., Wright, S.J.: Gradient projection for sparse reconstruction: application  
1063 to compressed sensing and other inverse problems. *IEEE J. Sel. Top. Signal Process.* **1**(4), 586–597 (2007)
- 1064 31. Franc, V., Hlavac, V., Navara, M.: Sequential coordinate-wise algorithm for the non-negative least squares  
1065 problem. In: Proceedings of the 11th International Conference on Computer Analysis of Images and  
1066 Patterns, pp. 407–414 (2005)
- 1067 32. Friedlander, M.P., Hatz, K.: Computing nonnegative tensor factorizations. *Comput. Optim. Appl.* **23**(4),  
1068 631–647 (2008)
- 1069 33. Frigyesi, A., Höglund, M.: Non-negative matrix factorization for the analysis of complex gene expression  
1070 data: identification of clinically relevant tumor subtypes. *Cancer Inform.* **6**, 275–292 (2008)
- 1071 34. Gillis, N.: Nonnegative matrix factorization complexity, algorithms and applications. Ph.D. thesis,  
1072 Université catholique de Louvain (2011)
- 1073 35. Gillis, N., Glineur, F.: Nonnegative factorization and the maximum edge biclique problem. CORE  
1074 Discussion Paper 2008/64, Université catholique de Louvain (2008)
- 1075 36. Gillis, N., Glineur, F.: Using underapproximations for sparse nonnegative matrix factorization. *Pattern*  
1076 *Recognit.* **43**(4), 1676–1687 (2010)
- 1077 37. Gillis, N., Glineur, F.: Accelerated multiplicative updates and hierarchical als algorithms for nonnegative  
1078 matrix factorization. *Neural Comput.* **24**(4), 1085–1105 (2012)
- 1079 38. Gillis, N., Glineur, F.: A multilevel approach for nonnegative matrix factorization. *J. Comput. Appl. Math.*  
1080 **236**, 1708–1723 (2012)
- 1081 39. Golub, G., Van Loan, C.: *Matrix Computations*. Johns Hopkins University Press, Baltimore (1996)
- 1082 40. Gonzalez, E.F., Zhang, Y.: Accelerating the lee-seung algorithm for non-negative matrix factorization.  
1083 Department of Computational and Applied Mathematics, Rice University, Technical report (2005)
- 1084 41. Grippo, L., Sciandrone, M.: On the convergence of the block nonlinear gauss-seidel method under convex  
1085 constraints. *Oper. Res. Lett.* **26**(3), 127–136 (2000)
- 1086 42. Han, L., Neumann, M., Prasad, U.: Alternating projected Barzilai-Borwein methods for nonnegative  
1087 matrix factorization. *Electron. Trans. Numer. Anal.* **36**, 54–82 (2009)
- 1088 43. Harshman, R.A.: Foundations of the parafac procedure: models and conditions for an "explanatory"  
1089 multi-modal factor analysis. In: *UCLA Working Papers in Phonetics*, vol. 16, pp. 1–84 (1970)
- 1090 44. Ho, N.D.: Nonnegative matrix factorization algorithms and applications. Ph.D. thesis, Univ. Catholique  
1091 de Louvain (2008)
- 1092 45. Horn, R.A., Johnson, C.R.: *Matrix Analysis*. Cambridge University Press, Cambridge (1990)
- 1093 46. Horst, R., Pardalos, P., Van Thoai, N.: *Introduction to Global Optimization*. Kluwer, Berlin (2000)
- 1094 47. Hoyer, P.O.: Non-negative matrix factorization with sparseness constraints. *J. Mach. Learn. Res.* **5**,  
1095 1457–1469 (2004)
- 1096 48. Hsieh, C.J., Dhillon, I.S.: Fast coordinate descent methods with variable selection for non-negative  
1097 matrix factorization. In: Proceedings of the 17th ACM SIGKDD International Conference on Knowledge  
1098 Discovery and Data Mining, pp. 1064–1072 (2011)
- 1099 49. Hutchins, L., Murphy, S., Singh, P., Graber, J.: Position-dependent motif characterization using non-  
1100 negative matrix factorization. *Bioinformatics* **24**(23), 2684–2690 (2008)
- 1101 50. Júdice, J.J., Pires, F.M.: A block principal pivoting algorithm for large-scale strictly monotone linear  
1102 complementarity problems. *Comput. Oper. Res.* **21**(5), 587–596 (1994)
- 1103 51. Kim, D., Sra, S., Dhillon, I.S.: Fast Newton-type methods for the least squares nonnegative matrix approxi-  
1104 mation problem. In: Proceedings of the 2007 SIAM International Conference on Data Mining, pp. 343–354  
1105 (2007)
- 1106 52. Kim, H., Park, H.: Sparse non-negative matrix factorizations via alternating non-negativity-constrained  
1107 least squares for microarray data analysis. *Bioinformatics* **23**(12), 1495–1502 (2007)

- 1108 53. Kim, H., Park, H.: Nonnegative matrix factorization based on alternating nonnegativity constrained least  
 1109 squares and active set method. *SIAM J. Matrix Anal. Appl.* **30**(2), 713–730 (2008)
- 1110 54. Kim, H., Park, H., Eldén, L.: Non-negative tensor factorization based on alternating large-scale non-  
 1111 negativity-constrained least squares. In: *Proceedings of IEEE 7th International Conference on Bioinformatics  
 1112 and, Bioengineering (BIBE07)*, vol. 2, pp. 1147–1151 (2007)
- 1113 55. Kim, J.: *Nonnegative Matrix and Tensor Factorizations, Least Squares Problems, and Applications*. Ph.D.  
 1114 Thesis, Georgia Institute of Technology (2011)
- 1115 56. Kim, J., Monteiro, R.D., Park, H.: Group Sparsity in Nonnegative Matrix Factorization. In: *Proceedings  
 1116 of the 2012 SIAM International Conference on Data Mining*, pp. 851–862 (2012)
- 1117 57. Kim, J., Park, H.: Sparse nonnegative matrix factorization for clustering. Technical report, Georgia  
 1118 Institute of Technology GT-CSE-08-01 (2008)
- 1119 58. Kim, J., Park, H.: Toward faster nonnegative matrix factorization: a new algorithm and comparisons. In:  
 1120 *Proceedings of the 8th IEEE International Conference on Data Mining (ICDM)*, pp. 353–362 (2008)
- 1121 59. Kim, J., Park, H.: Fast nonnegative matrix factorization: an active-set-like method and comparisons.  
 1122 *SIAM J. Sci. Comput.* **33**(6), 3261–3281 (2011)
- 1123 60. Kim, J., Park, H.: Fast nonnegative tensor factorization with an active-set-like method. In: *High-  
 1124 Performance Scientific Computing: Algorithms and Applications*, pp. 311–326. Springer (2012)
- 1125 61. Kolda, T.G., Bader, B.W.: Tensor decompositions and applications. *SIAM Rev.* **51**(3), 455–500 (2009)
- 1126 62. Korattikara, A., Boyles, L., Welling, M., Kim, J., Park, H.: Statistical optimization of non-negative matrix  
 1127 factorization. In: *Proceedings of the 14th International Conference on Artificial Intelligence and Statistics  
 1128 (AISTATS), JMLR: W&CP*, vol. 15, pp. 128–136 (2011)
- 1129 63. Kuang, D., Ding, C., Park, H.: Symmetric nonnegative matrix factorization for graph clustering. In:  
 1130 *Proceedings of 2012 SIAM International Conference on Data Mining*, pp. 106–117 (2012)
- 1131 64. Lawson, C.L., Hanson, R.J.: *Solving Least Squares Problems*. Prentice Hall, New Jersey (1974)
- 1132 65. LeCun, Y., Bottou, L., Bengio, Y., Haffner, P.: Gradient-based learning applied to document recognition.  
 1133 *Proc. IEEE* **86**(11), 2278–2324 (1998)
- 1134 66. Lee, D.D., Seung, H.S.: Learning the parts of objects by non-negative matrix factorization. *Nature*  
 1135 **401**(6755), 788–791 (1999)
- 1136 67. Lee, D.D., Seung, H.S.: Algorithms for non-negative matrix factorization. In: *Advances in Neural Informa-  
 1137 tion Processing Systems 13*, pp. 556–562. MIT Press (2001)
- 1138 68. Li, L., Lebanon, G., Park, H.: Fast bregman divergence nmf using taylor expansion and coordinate descent.  
 1139 In: *Proceedings of the 18th ACM SIGKDD international conference on Knowledge discovery and data  
 1140 mining*, pp. 307–315 (2012)
- 1141 69. Li, S.Z., Hou, X., Zhang, H., Cheng, Q.: Learning spatially localized, parts-based representation.  
 1142 In: *Proceedings of the 2001 IEEE Computer Society Conference on Computer Vision and, Pattern Recog-  
 1143 nition*, vol. 1, pp. I-207–I-212 (2001)
- 1144 70. Lin, C.: On the convergence of multiplicative update algorithms for nonnegative matrix factorization.  
 1145 *IEEE Trans. Neural Netw.* **18**(6), 1589–1596 (2007)
- 1146 71. Lin, C.J.: Projected gradient methods for nonnegative matrix factorization. *Neural Comput.* **19**(10),  
 1147 2756–2779 (2007)
- 1148 72. Lin, M.M., Chu, M.T.: On the nonnegative rank of euclidean distance matrices. *Linear Algebra Appl.*  
 1149 **433**(3), 681–689 (2010)
- 1150 73. Merritt, M., Zhang, Y.: Interior-point gradient method for large-scale totally nonnegative least squares  
 1151 problems. *J. optim. Theory Appl.* **126**(1), 191–202 (2005)
- 1152 74. Paatero, P., Tapper, U.: Positive matrix factorization: a non-negative factor model with optimal utilization  
 1153 of error estimates of data values. *Environmetrics* **5**(1), 111–126 (1994)
- 1154 75. Park, H., Kim, H.: One-sided non-negative matrix factorization and non-negative centroid dimension  
 1155 reduction for text classification. In: *Proceedings of the 2006 Text Mining Workshop in the Tenth SIAM  
 1156 International Conference on Data Mining* (2006)
- 1157 76. Pauca, V.P., Piper, J., Plemmons, R.J.: Nonnegative matrix factorization for spectral data analysis. *Linear  
 1158 Algebra Appl.* **416**(1), 29–47 (2006)
- 1159 77. Pauca, V.P., Shahnaz, F., Berry, M.W., Plemmons, R.J.: Text mining using non-negative matrix factoriza-  
 1160 tions. In: *Proceedings of the 2004 SIAM International Conference on Data Mining*, pp. 452–456 (2004)
- 1161 78. Schmidt, M.N., Winther, O., Hansen, L.K.: Bayesian non-negative matrix factorization. In: *Proceedings  
 1162 of the 2009 International Conference on Independent Component Analysis and Signal Separation, Lecture  
 1163 Notes in Computer Science (LNCS)*, vol. 5441, pp. 540–547. Springer (2009)
- 1164 79. Sra, S.: Block-iterative algorithms for non-negative matrix approximation. In: *Proceedings of the 8th  
 1165 IEEE International Conference on Data Mining*, pp. 1037–1042 (2008)
- 1166 80. Tibshirani, R.: Regression shrinkage and selection via the lasso. *J. R. Stat. Soc. Ser. B (Methodological)*  
 1167 **58**(1), 267–288 (1996)

- 1168 81. Van Benthem, M.H., Keenan, M.R.: Fast algorithm for the solution of large-scale non-negativity-  
1169 constrained least squares problems. *J. Chemom.* **18**, 441–450 (2004)
- 1170 82. Vavasis, S.A.: On the complexity of nonnegative matrix factorization. *SIAM J. Optim.* **20**(3), 1364–1377  
1171 (2009)
- 1172 83. Weinberger, K., Saul, L.: Distance metric learning for large margin nearest neighbor classification.  
1173 *J. Mach. Learn. Res.* **10**, 207–244 (2009)
- 1174 84. Welling, M., Weber, M.: Positive tensor factorization. *Pattern Recogn. Lett.* **22**(12), 1255–1261 (2001)
- 1175 85. Xu, W., Liu, X., Gong, Y.: Document clustering based on non-negative matrix factorization. In: Proceedings of the 26th Annual International ACM SIGIR Conference on Research and Development in  
1176 Informaion Retrieval, pp. 267–273 (2003)
- 1177 86. Zdunek, R., Cichocki, A.: Non-negative matrix factorization with quasi-newton optimization. In: Proceedings of the Eighth International Conference on Artificial Intelligence and, Soft Computing, pp. 870–879  
1178 (2006)
- 1179 87. Zdunek, R., Cichocki, A.: Fast nonnegative matrix factorization algorithms using projected gradient  
1180 approaches for large-scale problems. *Comput. Intell. Neurosci.* **2008**, 939567 (2008)
- 1181 88. Zhong, M., Girolami, M.: Reversible jump MCMC for non-negative matrix factorization. In: Proceedings of the Twelfth International Conference on Artificial Intelligence and Statistics (AISTATS), *JMLR: W&CP*, vol. 5, pp. 663–670 (2009)  
1182  
1183  
1184  
1185

Revised Proof